이학박사 학위논문

The role of bacteria in the pathogenesis of oral lichen planus and regulatory effect of estrogen on the physical barrier of oral epithelium

구강편평태선 병인에서 세균의 역할과 에스트로겐의 구강 상피 장벽 기능 조절 효과

2016년 2월

서울대학교 대학원

치의과학과 면역 및 분자미생물치의학 전공

최윤식

The role of bacteria in the pathogenesis of oral lichen planus and regulatory effect of estrogen on the physical barrier of oral epithelium

by

Yun Sik Choi

Under the supervision of

Professor Youngnim Choi, D.D.S., Ph. D.

A Thesis Submitted in Partial Fulfillment of

the Requirements for the Degree of

Doctor of Philosophy

February 2016

School of Dentistry

The Graduate School

Seoul National University

ABSTRACT

The role of bacteria in the pathogenesis of oral lichen planus and regulatory effect of estrogen on the physical barrier of oral epithelium

Yun Sik Choi

Immunology and Molecular Microbiology Major

Department of Dental Science

The Graduate School

Seoul National University

Background

Oral lichen planus (OLP) is a mucocutaneous disease of unknown etiology that results from T-cell mediated immune responses. Many factors, such as infectious agents, drugs, autoantigens, and dental materials, have been suggested as the specific antigens that are targeted by $CD8^+$ T cells. However, the exact etiopathogenesis of OLP is not known.

The microbial community of the host body is intimately associated with diverse host biological processes. Changes in human microbiota from a healthy state are associated with diverse localized or systemic diseases. However, the role of bacteria in the etiopathogenesis of OLP is not known.

The role of estrogen in the regulation of epithelial homeostasis, including the regulation of physical barriers and the host immune response, has been suggested by multiple lines of evidence. However, the role of estradiol on the regulation of homeostasis of gingival epithelia has not been studied.

The aim of study was to explore the role of bacteria in OLP and the regulatory effect of 17β-estradiol on gingival homeostasis.

Methods

The sections of oral mucosal biopsies, 36 OLP and 10 controls, were subjected to *in situ* hybridization, which was performed using a digoxigenin-labeled eubacterial probe targeting bacterial 16S rRNA. The presence of $CD4^+$, $CD8^+$ T cells, and macrophages were determined by the immunohistochemistry, and correlations between the levels of *in situ* bacteria and the levels of infiltrated cells were determined by Spearman's rho. In addition, dual detection of bacterial signals and CD8 was performed. Furthermore, the mucosal microbiota was analyzed by pyrosequencing the 16S rRNA and subsequent analysis.

Purified human $CD4^+$, $CD8^+$, and $CD14^+$ cells were infected with 5-(and 6-) carboxy-fluorescein diacetate succinimidyl ester (CFSE)-labeled bacteria, and the presence of bacteria inside those cells was confirmed via confocal microscopy and flow cytometry. In addition, an antibiotics protection

assay was performed. Furthermore, the amounts of secreted chemokines were analyzed by ELISA and multiplex assay.

Confluent monolayers of immortalized human oral keratinocyte (HOK-16B) cells were treated with 17β-estradiol. The transepithelial electrical resistance (TER) was measured at various time points. Furthermore, the levels of TJ proteins were confirmed by real-time RT-PCR or immunofluorescence (IF). In addition, the nuclear factor kappa-light-chain-enhancer of activated B cells (NF-κB) nuclear translocation was confirmed by IF.

Results

In the oral mucosa, positive signals of bacteria were detected within the lamina propria and the epithelia, and the bacterial invasion into lamina propria was significantly increased in OLP patients. The levels of $CD4^+$ and $CD8^+$ T cells but not those of macrophages had a strong positive correlation with the levels of bacteria detected within the lamina propria. In addition, bacterial signals were observed within $CD8^-$ and $CD8^+$ T lymphocytes.

Oral bacterial communities in OLP patients were substantially different compared to healthy subjects. At the species levels, the relative abundances of 42 species were significantly different between healthy and OLP patients. *C. gingivalis* was significantly associated with increased OLP risk, and induced a significant decrease in TER in a time dependent manner without affecting the viability of HOK-16B cells. All selected bacteria were detected within $CD4^+$,

$CD8^+$, and $CD14^+$ cells after 1 h of infection. However, only *C. gingivalis* could survive within $CD14^+$ cells for 24h. All selected bacteria-induced chemokines have been implicated in OLP.

Under normal conditions, 17β-estradiol enhanced the epithelial physical barrier and induced increased levels of TJ proteins. Furthermore, pretreatment of 17β-estradiol protected against the disruption of the epithelial physical barrier function through the maintenance of TJ protein expression. In addition, 17β-estradiol inhibited NF-κB nuclear translocation via pro-inflammatory cytokine TNF-α.

Conclusion

In conclusion, increased bacterial invasion into mucosal cells/tissues and altered microbial communities may contribute to the etiopathogenesis of OLP. Maintaining the epithelial physical barrier could be targeted by 17β-estradiol to prevent bacterial invasion into tissues and reduce the occurrence of OLP.

Keywords: Oral lichen planus, Physical barrier, Inflammation, Bacterial invasion, Estrogen, Anti-inflammatory effect

Student number: 2010-30658

CONTENTS

Chapter I. Introduction

1.1. Oral lichen planus

Oral lichen planus (OLP) is a mucocutaneous disease of unknown etiology resulting from T-cell-mediated immune responses. Approximately 2% of the general population are affected by this disease (Thornhill et al., 2006). OLP is observed bilaterally on the buccal mucosa, the gingiva, and the tongue (Fig.1). OLP is classified into several types, including reticular and erosive OLP. The most common type of OLP is a reticular form that presents white keratotic striations with an erythematous region (Sugerman and Savage, 2002). The second most common type is erosive OLP presenting erythematous region and ulceration surrounded by radiating striae (Sugerman and Savage, 2002). When characteristic skin lesions are present, the diagnosis of OLP can be made with more confidence (Edwards and Kelsch, 2002).

Figure 1. Oral lichen planus involving the buccal mucosa and tongue.

The histopathological features of OLP include the liquefaction of the basal layer of the epithelia, band-like lymphocytic infiltration at the interface between the epithelia and submucosa, and degenerating keratinocytes (called as civatte bodies) (Sugerman and Savage, 2002; Thornhill et al., 2006). The infiltrated lymphocytes are mainly $CD4^+$ and $CD8^+$ T cells, and $CD8^+$ T cells are regarded as able to mediate the degeneration/destruction of epithelial cells (Iijima et al., 2003; Sugerman and Savage, 2002). Many factors such as infectious agents, drugs, autoantigens, and dental materials have been suggested as specific antigens that are targeted by the $CD8^+$ T cells (Iijima et al., 2003). Because the etiopathogenesis of OLP remains unclear, corticosteroid is widely used in the treatment of OLP (Edwards and Kelsch, 2002).

Oral lichenoid lesions (OLL) are regarded as variants of OLP and are often indistinguishable in symptoms. OLL is caused by certain medications or dental materials or as a manifestation of graft-vs-host disease (Edwards and Kelsch, 2002; Iijima et al., 2003). OLL lesions disappear after eliminating exposure to etiological factors. The histopathological features of OLL are not specific to one disease (Sugerman and Savage, 2002), and the essential features of OLL are damage to the basal keratinocytes including apoptosis, infiltrated inflammatory cells in the lamina propria, and hyperkeratosis (Ismail et al., 2007; McParland and Warnakulasuriya, 2012). These features are seen

in diverse oral diseases such as OLP, OLL, discoid lupus erythematosis (DLE), erythema multiforme, and graft-vs-host disease (Ismail et al., 2007). The World Health Organization (WHO) presented the criteria of the clinical and histopathological diagnosis of OLP. However, the validity of an OLP diagnosis has not been tested, and there are no agreed upon criteria to distinguish the histopathological features between OLP and OLL (Thornhill et al., 2006). Therefore, making clinical and histological distinctions between OLL and OLP is difficult due to the lack of differential biomarkers.

1.2. Pilot study: Relationship between bacterial invasion and immune cell infiltration in periodontitis

OLP has something in common with periodontitis. First, OLP is a chronic inflammatory disease. Second, OLP involves the degeneration/destruction of epithelial cells, indicating the disruption of the physical barrier. Third, OLP occurs in the oral cavity, which is exposed to more than 1000 bacterial species that form a biofilm. Based on the lessons learned from the study of periodontitis, this study would apply a pathogenesis model that includes the relationship between oral bacteria, the physical barrier, and inflammatory infiltration.

1.2.1. Periodontitis and dysbiosis of plaque biofilm

The human oral cavity is colonized by more than 1000 bacterial species (Wade, 2013). The gingival pocket is a unique interface between hard and soft tissue; oral bacteria colonize the hard tissues and form dental plaque in the gingival pocket (Matthews et al., 2007). Although some bacteria can lead to harmony with the host, certain bacteria called periodontal pathogens induce the disruption of homeostasis between bacteria and the host (Feng and Weinberg, 2006; Roberts and Darveau, 2002). Socransky classified these plaque-associated bacteria into six bacterial complexes: purple, yellow, green, orange, red, and *Actinomyces* (Socransky et al., 1998) (Fig. 1). In addition, Socransky found that the purple, yellow, green, and *Actinomyces* complexes consist of bacteria that are primary colonizers, the orange complex consists of bacteria that are bridging colonizers, and the red complex consists of bacteria that are late colonizers (Socransky et al., 1998).

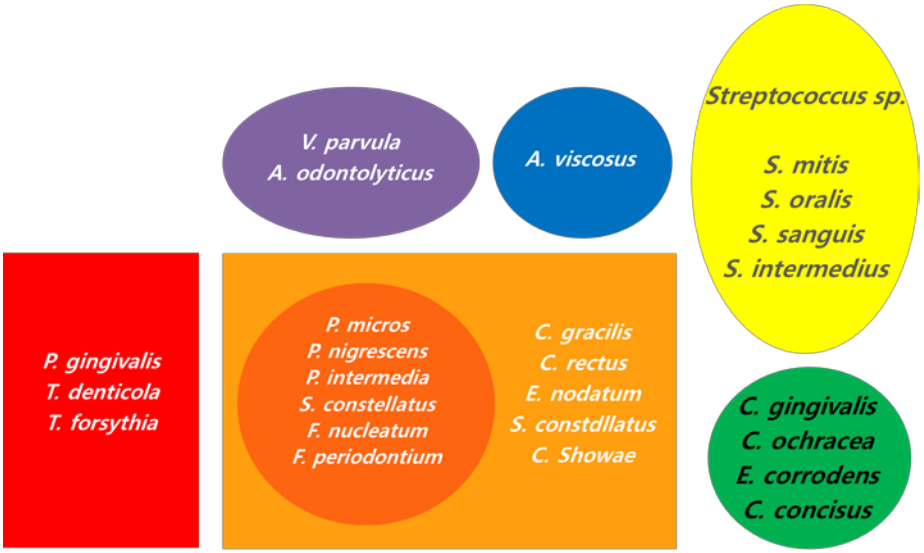

Figure 2. Classification of subgingival microbiota by Socransky (Socransky et al., 1998).

The microbial community of the human body is intimately associated with diverse host biological process such as tissue development, immune response, and metabolism (Cho and Blaser, 2012; Galimanas et al., 2014; Pflughoeft and Versalovic, 2012). Changes in human microbiota from a healthy state are associated with diverse localized or systemic diseases (Cho and Blaser, 2012). Periodontitis is a major chronic inflammatory disease caused by the dysbiosis of subgingival microbiota (Galimanas et al., 2014). The initiation and progression of periodontitis is triggered by two events, and includes an increased number and altered composition of the oral microbiota

(Listgarten, 1988; Loe et al., 1978). Increased levels of red complex bacteria including *Porphyromonas gingivalis*, *Tannerella forsythia*, and *Treponema denticola* from dental plaque during the transition from health to periodontitis indicate that they have important roles in the onset and progression of periodontitis (Socransky et al., 1998). In particular, *P. gingivalis*, the so-called keystone pathogen of periodontitis, has been shown to induce dysbiosis in homeostatic benign microbiota in animal models (Hajishengallis et al., 2011).

1.2.2. Types of bacteria and virulence factors involved in periodontitis

The characteristics of red complex bacteria were widely studied. *P. gingivalis* produces diverse virulence factors as destructing enzymes, including trypsin like-protease, aminopeptidase, alkaline phospholipase, collagenase, and phospholipase A (Holt et al., 1999; Murakami et al., 2004; Nakayama, 2003). Lipopolysaccharides (LPS), hemagglutinins, and fimbriae are also virulence factors of *P. gingivalis* (Holt et al., 1999). *P. gingivalis* has the ability to evade host immune responses such as the inhibition of phagocytosis, degradation of iron transport proteins, complements, and cytokines (Holt et al., 1999). *T. denticola* is a well-known periodontal pathogen. Virulence factors of *T. denticola* are LPS, outer surface proteins, peptidoglycan, and proteolytic

enzyme (Ishihara and Okuda, 1999; Masuda and Kawata, 1982; Sela, 2001). *T. denticola* can suppress phagocytosis by neutrophils and the proliferation of fibroblasts. In addition, this pathogen can hydrolyze various cytokines and chemokines via dentisilin (Boehringer et al., 1984; Ji et al., 2007). *T. forsythia* has potent virulence factors, including secreted protein BSA, components of the bacterial surface (S)–layer, hamagglutinin, and trypsin-like proteins (Sharma, 2010). In addition, *T. forsythia* is resistant to antimicrobial peptide LL-37 and neutrophil phagocytosis (Ji et al., 2007).

1.2.3. Epithelial barrier against invading bacteria

The gingival tissue is in constant close contact with plaque-associated bacteria. Therefore, the gingival epithelia form a barrier between plaque-associated bacteria and gingival tissue, providing the first line of defense against invading bacteria. The epithelial barrier consists of physical, chemical, and immunological barriers (Fig. 3). First, gingival epithelial cells are adjoined by tight junction (TJ)-related structures, and adhering junctions (AJ) form the unique architectural integrity of the stratified epithelia, which provides a physical barrier (Franke and Pape, 2012; Hatakeyama et al., 2006). **Second**, a variety of antimicrobial peptides such as human beta defensins and LL-37 that are secreted by epithelial cells form a chemical barrier (Dale and Fredericks,

2005). **Third**, the immunological barrier of gingival epithelia is composed of T cells, dendritic cells, macrophages, mast cells, and neutrophils that are distributed within the epithelia, lamina propria, and/or gingival sulcus (Page, 1986). The importance of chemical barriers is also evident in patients with Kostmann syndrome, who lack LL-37 in their saliva and neutrophils and develop severe periodontitis in young adulthood (Nussbaum and Shapira, 2011). However, the role of physical barriers in the pathogenesis of periodontitis has not been studied.

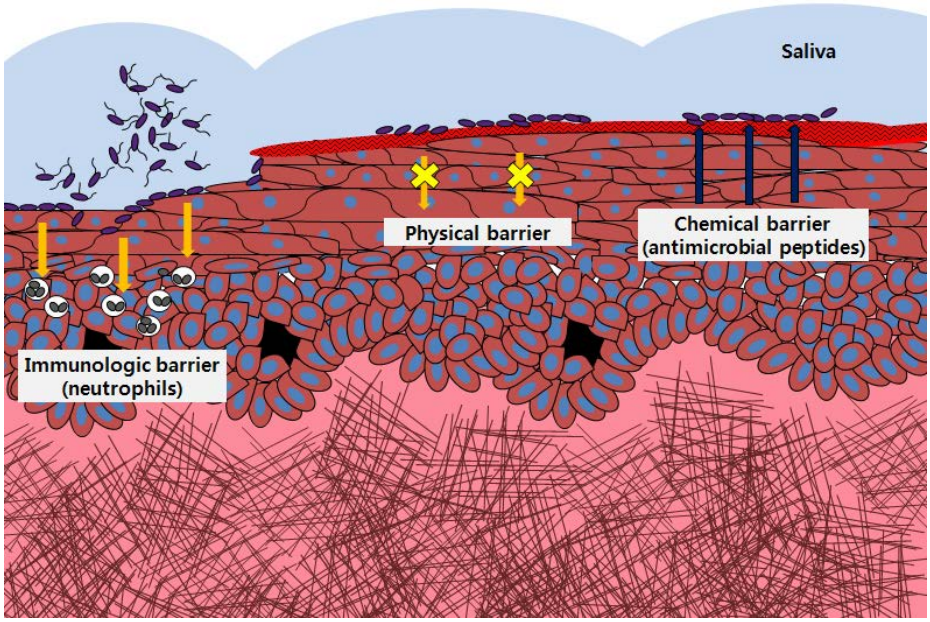

Figure 3. Epithelial barrier against invading bacteria

There are two types of cell junctions associated with physical barrier (Giepmans and van Ijzendoorn, 2009) (Fig. 4). AJs initiate cell–cell adhesion,

and provide anchoring strength below tight junctions. In addition, they regulate cytoskeleton organization and intracellular signaling. AJs are regulated by the cadherin superfamily, such as E-cadherin and catenin family members including β-catenin, and α-catenin (Hartsock and Nelson, 2008). Although the assembly of TJs require the formation of AJs, E-cadherin is not required for the organization of TJs (Hartsock and Nelson, 2008; Niessen, 2007). TJs act as a barrier to the paracellular translocation of particles and molecules (Giepmans and van Ijzendoorn, 2009; Niessen, 2007). TJs are regulated by transmembrane proteins such as junctional adhesion molecules (JAMs), occludins, claudins, and associated cytoplasmic proteins zonula occludens (ZOs). ZO-1, ZO-2, and ZO-3 are a membrane-associated guanylate kinase homologs (MAGUK) family that includes binding domains to the proteins of AJs, TJs, and actin cytoskeleton (Hartsock and Nelson, 2008; Niessen, 2007). ZOs are scaffolding proteins that link other TJ proteins to the actin cytoskeleton (Hartsock and Nelson, 2008; Niessen, 2007). The function of the physical barrier is associated with the expression levels and localization of TJ proteins.

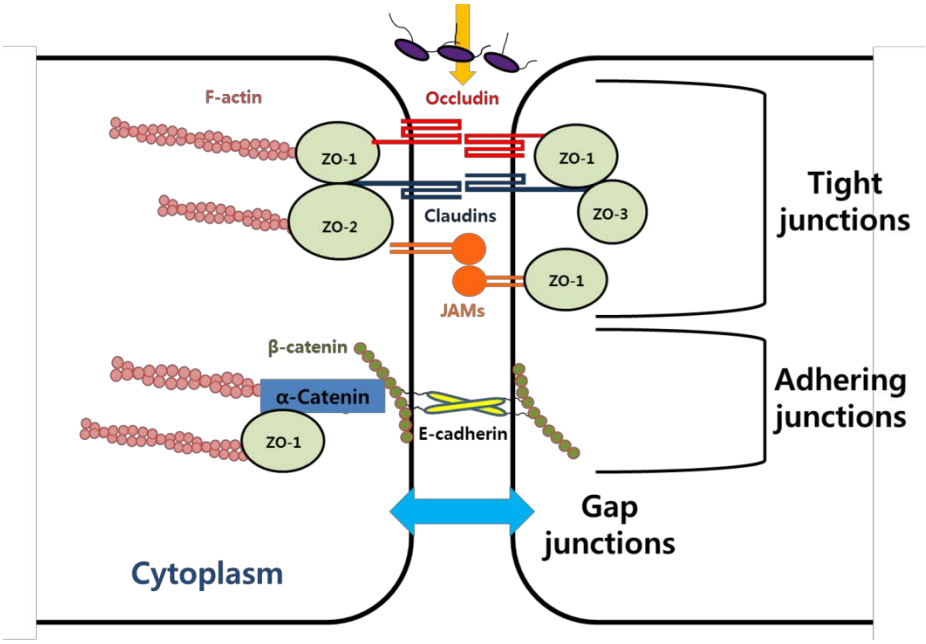

Figure 4. Adhering and tight junctions

1.2.4. Invasion of pathogenic bacteria into the oral epithelial cells

Periodontal pathogens such as *P. gingivalis*, *T. forsythia*, *A. actinomycetemcomitans*, and *T. denticola* have the ability to invade epithelial cells (Lamont and Yilmaz, 2002; Meyer et al., 1996; Njoroge et al., 1997; Shin and Choi, 2012). The initial interaction between bacterial ligands and epithelial cells causes a rearrangement of cellular components, which provides pathogen entry into non-phagocytic epithelial cells (Lamont et al., 1995). An invasion of *P. gingivalis* into host cells is initiated when major fimbriae bind to the integrin β1 integrin receptor, which results in a signaling cascade for the

remodeling of the cytoskeleton to enable pathogen entry (Yilmaz et al., 2002). Another periodontal pathogen *T. forsythia* invades epithelial cells by using bacterial surface protein (Bsp) A, which requires clathrin-mediated endocytosis and a phosphoinositide 3-kinase (PI3K) signaling cascade (Mishima and Sharma, 2011). In addition to the *in vitro* intracellular invasion of periodontal pathogens, the presence of bacteria within the gingival tissues of periodontal lesions has been repeatedly reported (Choi et al., 2013; Kim et al., 2010), suggesting an important role of bacterial invasion in the pathogenesis of periodontitis.

1.2.5. Modulation of epithelial TJ-related structures by pathogenic bacteria

Many pathogenic bacteria are known to modulate epithelial physical barriers, particularly TJ proteins such as JAMs, ZOs, occludin, and claudins, to enter host cells and/or tissues (Dickman et al., 2000; Nusrat et al., 2001; Wu et al., 2000). Inflammatory bowel disease, a chronic inflammatory disorder of the gastrointestinal tract caused by a disruptive interaction between the immune system and gut microbes, is associated with barrier dysfunction and increased epithelial permeability (Salim and Soderholm, 2011). Indeed, periodontal pathogens such as *P. gingivalis*, *T. denticola*, and *A. actinomycetemcomitans*

induce damage or remodeling of TJs and AJs of gingival epithelial cells *in vitro*, and the involvement of virulence factors such as gingipain, dentilisin, and cytolethal distending toxin has been shown (Cereijido et al., 2007; Chi et al., 2003; Katz et al., 2002).

1.2.6. Pathogenesis of periodontitis based on the previous study

In the previous studies (Choi et al., 2013; Choi et al., 2014), dextran sulfate sodium (DSS), a TJ-disrupting chemical, was applied onto gingival mucosa of mice in the absence or presence of *P. gingivalis* to investigate the role of physical barriers in the pathogenesis of periodontitis. The levels of the TJ protein ZO-1, the number of T cells, and the presence of bacteria within the gingival tissue were examined by immunohistochemistry and *in situ* hybridization, respectively. In addition, oral bacteria communities were analyzed via pyrosequencing.

Previous studies (Choi et al., 2013; Choi et al., 2014) showed that (1) DSS induces periodontitis in mice and that DSS- or *P. gingivalis*-induced impairment of TJ facilitated the invasion of oral bacteria and T cell infiltration into the gingival tissues. (2) The expression levels of ZO-1 are decreased and, the bacterial invasion of gingival tissue is increased in lesions of periodontitis

patients. (3) Both DSS application and *P. gingivalis* inoculation can induce dysbiosis of oral microbiota in mouse.

Decreased levels of TJ proteins ZO-1 by both *P. gingivalis* and DSS in the gingival epithelia

The physical barrier function is associated with the expression levels and distribution of TJ proteins. *P. gingivalis* infection altered the distribution of ZO-1 proteins and induced the rounding of cells, leading to the detachment of cell-to-cell contacts (Fig. 5a-b). DSS treatment also reduced overall levels of ZO-1 expression (Fig. 5a-b). Interestingly, mice from the DSS or *P.gingivalis* infection showed significantly reduced expression of ZO-1 in the junctional epithelia (Fig. 5c-d).

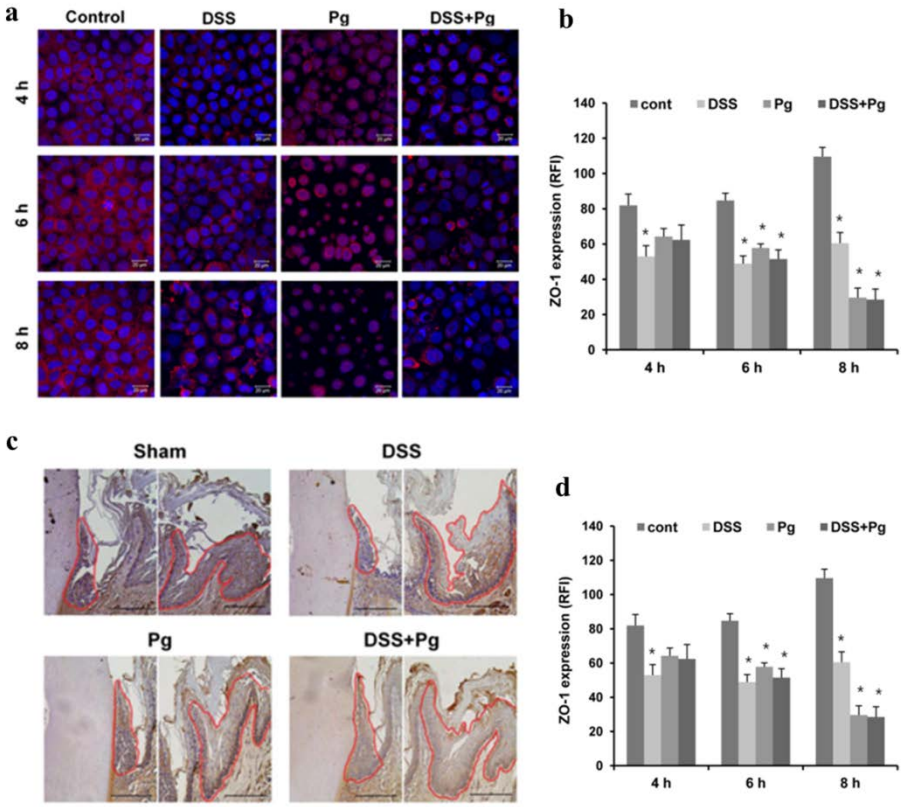

Figure 5. Decreased levels of TJ proteins ZO-1 by both *P. gingivalis* and DSS in the gingival epithelia. a-b) HOK-16B cells were plated and grown until a confluent monolayer. The cells were treated with vehicle, DSS (dextran sulfate sodium), *P. gingivalis* (Pg), or DSS+Pg for 4, 6, or 8 h. After fixation, the cells were stained for ZO-1 and examined by confocal microscopy. The fluorescence intensity of ZO-1 was analyzed by Zen 2010 software and normalized to the DAPI intensity. c-d) Six-week-old Balb/c mice received an applications of 5% DSS onto the gingival mucosa (DSS),

inoculation with *P. gingivalis* (Pg), both (DSS+Pg), or vehicles alone. Gingival tissues from mice were stained for ZO-1 by immunohistochemistry (scale bar = 100 μm at 400 x). The mean intensity of ZO-1 per region of interest was analzed by ImageJ software. *, $P < 0.05$ (Mann-Whitney U test).

Increased bacterial invasion within the gingival tissues by both *P. gingivalis* inoculation and DSS treatment

Bacterial invasion within gingival tissues is associated with pathogenesis of periodontitis. When the number of invasion was counted, bacterial invasion was increased by *P. gingivalis* inoculation. Interestingly, DSS treatment alone also induced increased bacterial invasion within gingival tissues (Fig. 6).

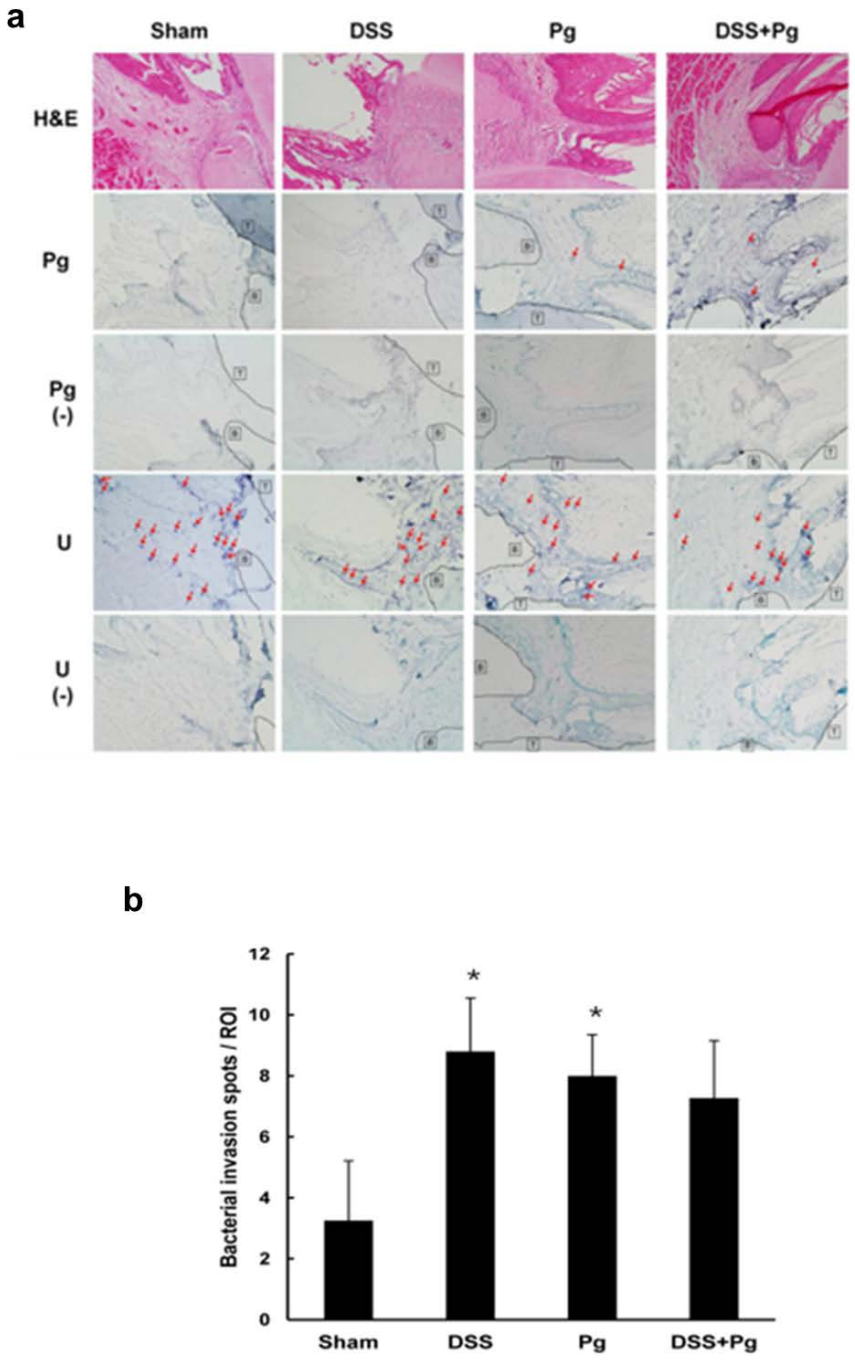
a
Sham
DSS
Pg
DSS+Pg
H&E
Pg
Pg
(-)
U
U
(-)
b
Bacterial invasion spots / ROI
12
10
8
6
4
2
0
*
*
Sham
DSS
Pg
DSS+Pg

Figure 6. Increased bacterial invasion within the gingival tissues by both *P. gingivalis* inoculation and DSS treatment. a-b) Gingival tissues from mice were stained with hematoxylin-eosin or in situ hybridized with either *P. gingivalis*-specific probe (Pg) or a universial probe (U). Hybridization was also performed with each probe mixed with 10-fold excess unlabeled probe as a negative control (-). Positive signals are marked with arrows. The numbers of positive signals of universal probe were counted. *, $P < 0.05$ (Mann-Whitney U test).

Decreased levels of TJ proteins and increased bacterial invasion in the periodontal lesions of patients with periodontitis

The expression levels of ZO-1 were decreased in the periodontal lesion (Fig. 7a). In addition, the bacterial invasion of gingival tissue was increased in periodontal lesions compared with healthy sites (Fig. 7b). Indeed, bacterial invasion was inversely associated with the levels of ZO-1 in both periodontitis animal model (r = -0.252, P = 0.139) and human periodontitis (r = -0.287, P = 0.07). *, $P < 0.05$ (Mann-Whitney U test).

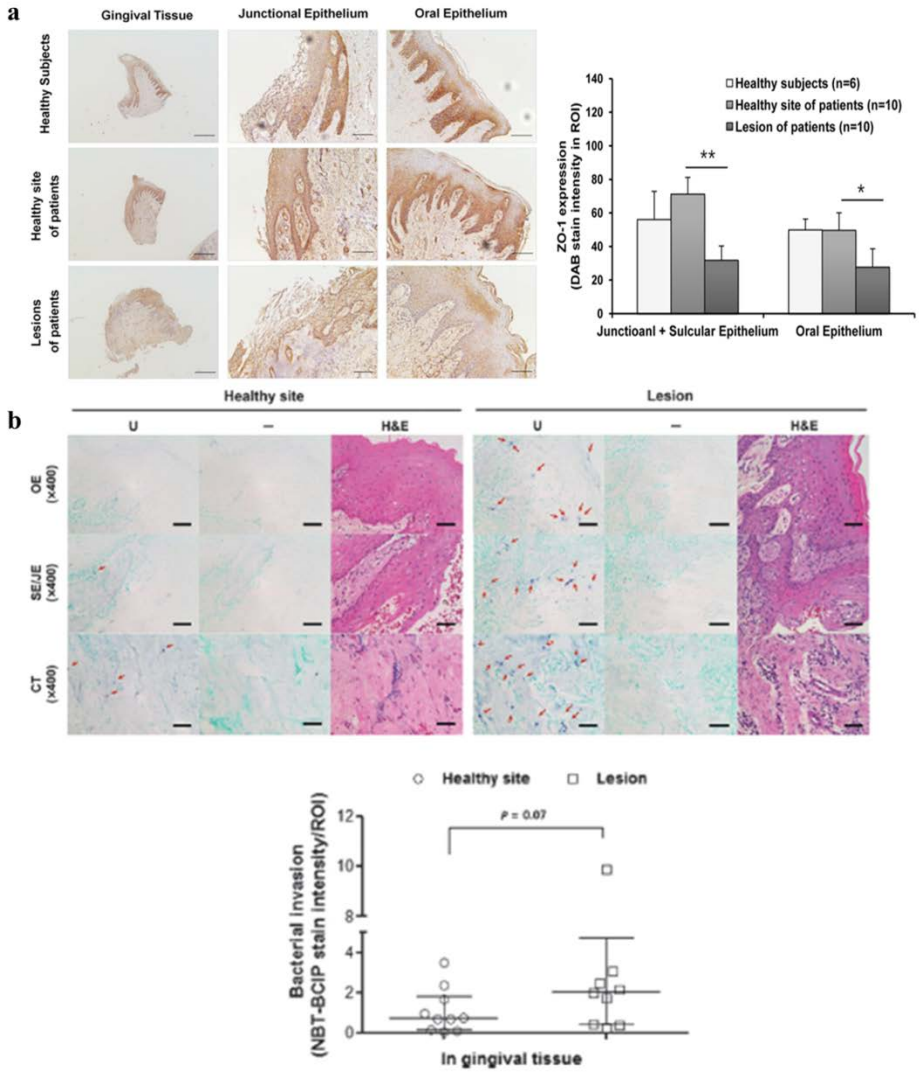

Figure 7. Decreased levels of TJ proteins and increased bacterial invasion in the periodontal lesions of patients with periodontitis. a) Gingival tissues from healthy subject and patients with chronic periodontitis were stained with ZO-1 by immunohistochemistry (scale bar = 500 μm at 100 x , 100 μm at

400 x). The stained signals per region of interest were analyzed using ImageJ software. b) Gingival tissues from patients with chronic periodontitis were stained with hematoxylin-esoin (H&E) or *in situ* hybridized with a universal probe (U). The oral epithelium (OE), sulcular/junctional epithelium (SE/JE), and connective tissues (CT) were photographed (scale bar = 50 μm). The stained bacterial signals per region of interest were analyzed using ImageJ software. *, $P < 0.05$; **, $P < 0.01$ (Mann-Whitney U test).

A strong positive correlation between bacterial invasion and T cell infiltration

Bacterial invasion within gingival tissues drives inflammatory infiltrate. The numbers of T cells detected in the gingival tissues were increased in all of the experimental groups (Fig. 8). Notably, the number of T cells had a strong positive correlation with the number of bacteria. In addition, bacterial signals from gingival tissues of human periodontitis patients were detected near to the infiltrated immune cells (Fig. 8). Therefore, these data indicate that defect of epithelial physical barrier allows bacterial invasion into the tissues and concurrent chronic inflammation.

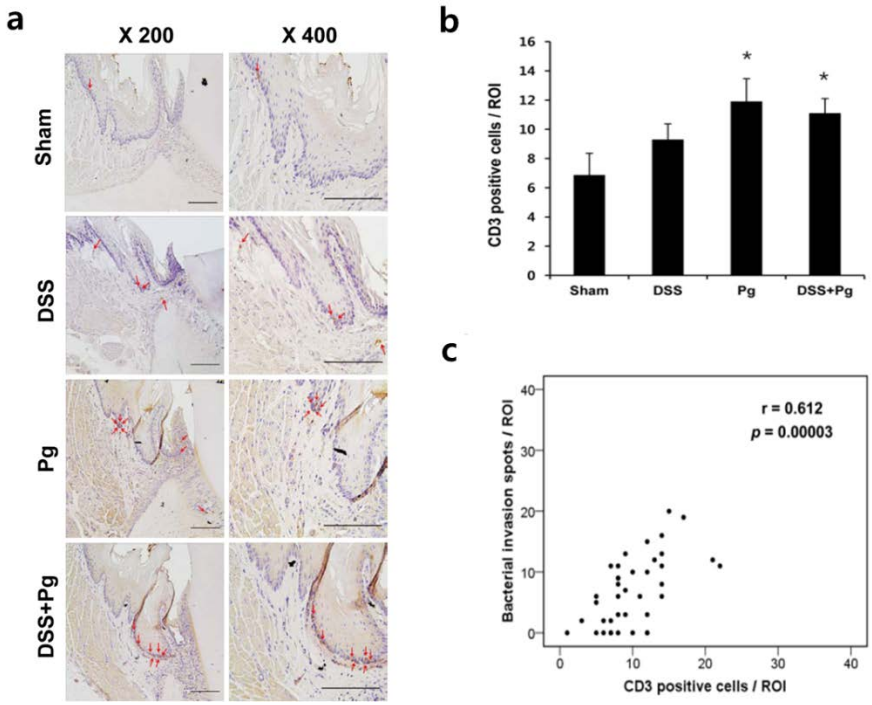

Figure 8. A strong positive correlation between bacterial invasion and T cell infiltration. a) Gingival tissues from mice were stained for CD3 by immunohistochemistry (scale bar = 200 μm). CD3-positve cells are indicated with arrows. b) The numbers of CD3-positive cells were counted at gingival tissues. *, $P < 0.05$ (Mann-Whitney U test). c) Two-tailed Spearmas's rank correlations between the number of CD3-positive cells and bacterial invasion are shown.

Dysbiosis of oral microbiota by both *P. gingivalis* inoculation and DSS treatment

Human periodontitis is associated with a microbial shift in the indigenous oral flora (Galimanas et al., 2014). Although many changes were not observed at the phylum levels, dysbiosis of the bacterial community was evident in all experimental groups (Fig. 9). This data indicates that not only pathogen could trigger dysbiosis of microbiota, but also the altered characteristics of the epithelial environment could induce microbial shift.

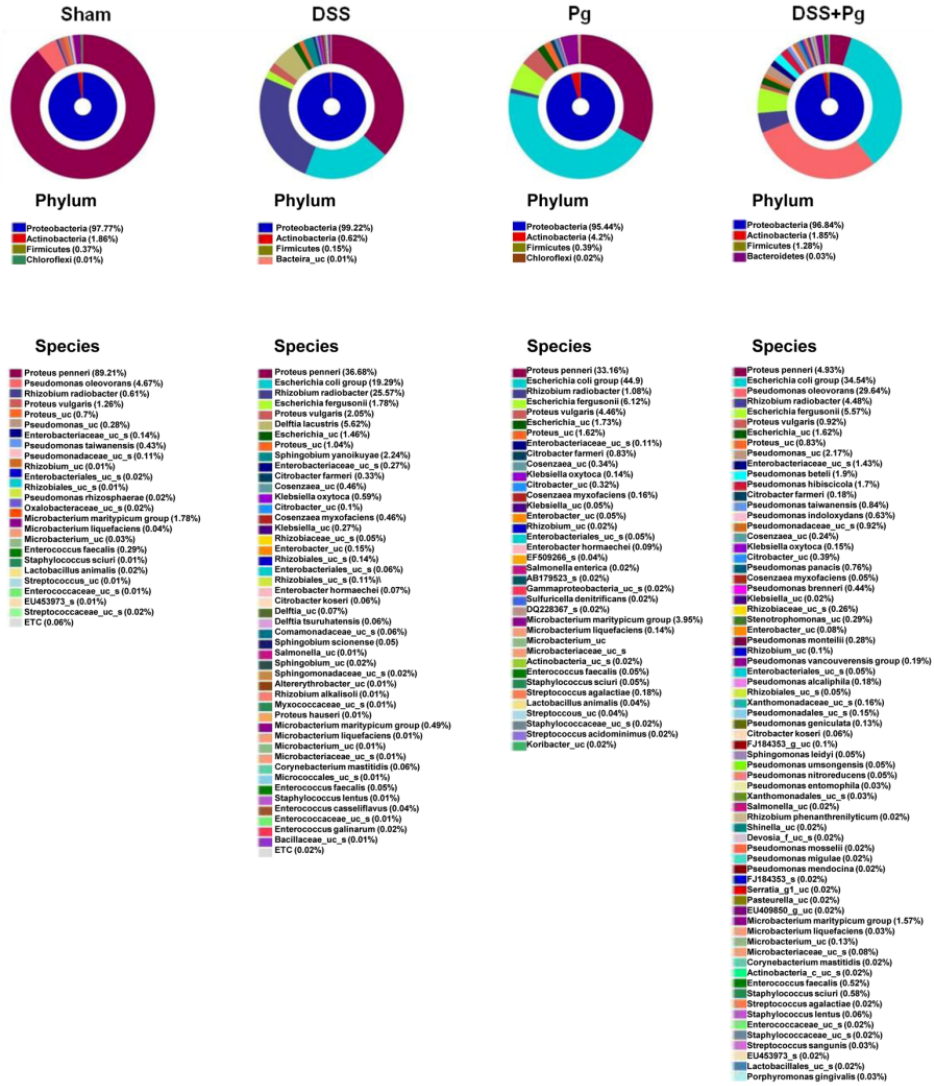

Figure 9. Dysbiosis of oral microbiota by both *P. gingivalis* inoculation and DSS treatment. The bacterial DNA obtained from multiple mouse were

pooled for each group. The bacterial communities of pooled DNA samples were analyzed by pyrosequencing of amplified 16S rRNA fragments. The composition of oral microbiota at the phylum and species are shown.

Expression patterns of growth factor receptors in the human gingival epithelia

Because epithelial physical barrier provides first defense line against invading bacteria, the maintenance of epithelial homeostasis is important. Among the growth factors that control epithelium homeostasis, epidermal growth factor (EGF), keratinocyte growth factor (KGF, also known as fibroblast growth factor 7), and insulin-like growth factor-I (IGF-I) have been implicated in the regulation of TJ proteins and paracellular permeability in lung and/or intestinal epithelia. However, the result of pilot study (Choi et al., 2014) show that almost growth factor receptor were expressed in the basal layer of gingival epithelia (Fig. 10).

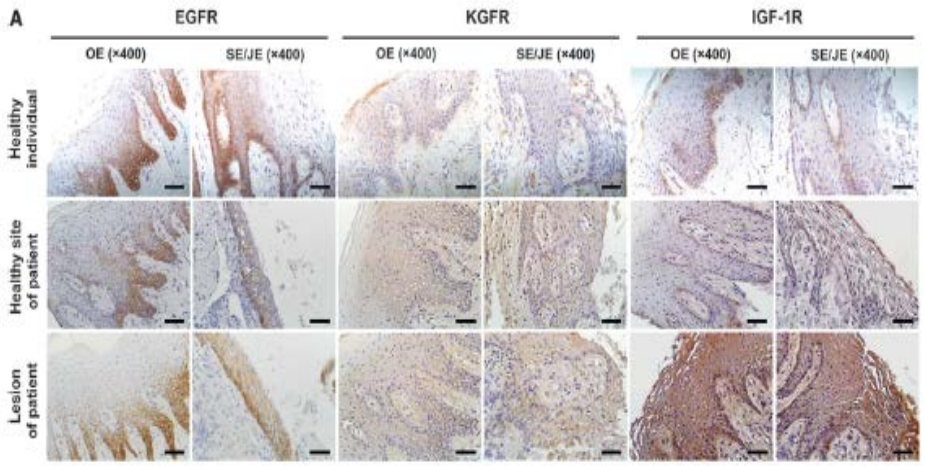

Figure 10. Expression patterns of growth factor receptors in the human gingival epithelia. These gingival tissues were obtained from patients who had undergone periodontal surgery. Gingival tissues from nine patients were acquired during resective periodontal surgeries. When the resective surgery was performed, incision lines had to be extended into the non-inflamed adjacent tissue to gain access into the bottom of deep periodontal pockets. The gingival tissues were separated into healthy sites (n = 10) with no feature of inflammation (pocket depth [PD] ≤3mm and negative bleeding on probing [BOP] and periodontal lesions (n = 10) showing signs of tissue breakdown (mean PD: 5.2 mm) and inflammation, i.e., redness, BOP, and swelling. The expression of EGF receptor (EGFR), KGF receptor (KGFR), and IGF-1 receptor (IGF-1R) were evaluated in gingival tissues from healthy and diseased sites in patients with periodontitis by immunohistochemistry. The

oral epithelium (OE) and sulcular/junctional epithelium (SE/JE) were photographed (scale bar = 50 μm).

1.3. Estrogen

1.3.1. Steroid hormone

There are two types of steroid hormone: adrenocortical and sex hormones (Nussdorfer et al., 1999). Because forms of steroid hormones are lipid, they can penetrate the cell membrane (Yang et al., 2014). Steroid hormones are synthesized in the adrenal cortex and gonads (testes and ovaries) from cholesterol; however, steroid hormones can also be produced by peripheral conversion in local tissues such as the liver and fat (Wierman, 2007). The cyclopentanoperhydrophenanthrene nucleus is the basic structure of these hormones (Fig. 11). Although the overall structure of steroid hormones is similar, each receptor can be highly specific. The basic classification of steroid hormones is classifying them by the number of carbons in their structures (Norman et al., 2004).

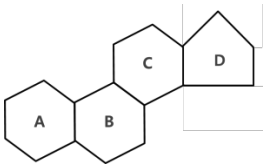

Figure 11. cyclopentanoperhydrophenanthrene.

1.3.2. Biosynthesis of steroid hormone

Pregnenolone and progesterone are requisites for the synthesis of all steroid hormones. Cholesterol is converted to pregnenolone via side chain cleavage. The 3β-hydroxysteroid dehydrogenase and $\Delta^{4,5}$-isomerase convert pregnenolone to progesterone. The pathway for the biosynthesis of steroid hormones is presented in Figure 12. Progesterone is converted to aldosterone in the adrenal zona glomerulosa cells by the 21β-hydroxylase of the endoplasmic reticulum and 11β- hydroxylase and 18β- hydroxylase of the mitochondria. 17β-hydroxylase and 21β-hydroxylase of endoplasm reticulum with 18β-hydroxylase are required in the synthesis of cortisol. 17-dehydrogenase converts progesterone to testosterone, which is a major product of the Leydig cells of the testis, and is converted to dihydrotestosterone by the 5α-reductase of endoplasmic reticulum and nucleus. Dihydrotestosterone, weak androgen, can be converted to testosterone through androstenedione, and testosterone is converted to estradiol by the aromatase system (Devlin and Wiley-Liss, 2006).

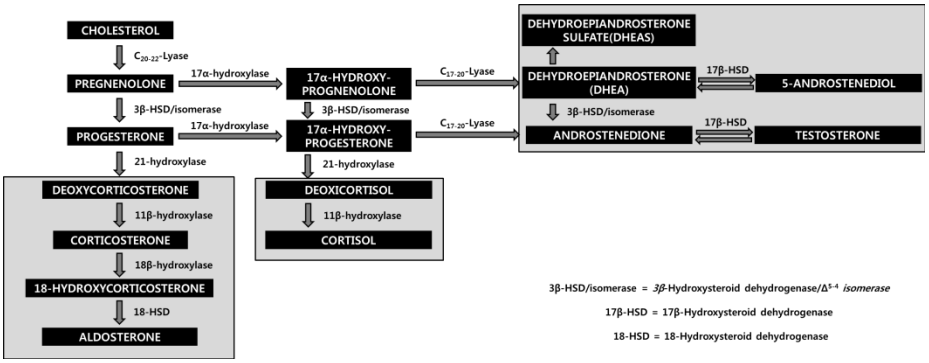

Figure 12. The pathway for the biosynthesis of steroid hormones.

1.3.3. Estrogen

Sex steroid hormones including estrogens, androgens, and progestins have a role in normal reproductive function and secondary sex characteristics. Estrogens are female hormones produced by the ovaries, but they are also produced by local target cells (Wierman, 2007). Estrogens are classified into three common classes: estrone (E1), estradiol (E2), and estriol (E3). Estradiol is the most powerful and common class of estrogen (Devlin and Wiley-Liss, 2006). The functions of estrogen are mediated through two types of nuclear receptors: estrogen receptor-α (ERα) and estrogen receptor-β (ERβ). After binding to estrogens, ER induces gene transcription via the dissociation of receptor-associated proteins (Esposito, 1991). The actions of ERα are involved in classical effects such as the regulation of the menstrual cycle and secondary sex characteristics in females and the maturation of sperm in males,

whereas ERβ is involved in a minor role in certain estrogen target tissues (Looijer-van Langen et al., 2011).

Multiple studies have reported that changes of estrogen status in the duration of the menstrual cycle, pregnancy, and puberty are associated with the occurrence of gingivitis (Carrillo-de-Albornoz et al., 2012; CB and NF, 2006; Oh et al., 2002). In addition, estrogen deficiency is considered a risk factor for periodontitis (Haas et al., 2009). Estrogen treatment improves disease status in high-fat diet (HFD)-induced periodontitis animal model (Blasco-Baque et al., 2012). Moreover, the replacement of estrogen leads to a decreased number of periodontal pathogens in post-menopausal women and HFD-induced periodontitis animal model (Blasco-Baque et al., 2012; Tarkkila et al., 2010). Furthermore, estrogen modulates physical barrier functions and inflammatory responses in diverse epithelial cells (Chotirmall et al., 2010; Liu et al., 2005; Looijer-van Langen et al., 2011; Schaefer et al., 2005). However, the role of estrogen on the regulation of gingival epithelial homeostasis has not yet been studied.

Although almost all growth factor receptors were expressed in the basal layer of gingival epithelia (Choi et al., 2014) (Fig. 10), ERβ is expressed throughout all layers of the oral epithelia (Valimaa et al., 2004). Because estradiol is lipid-soluble, its usage would be more effective than growth factors.

1.4. Aim of the present study

Based on the lessons learned from the previous study regarding periodontitis, the present study hypothesized that bacterial invasion into the mucosal tissue may be the cause of the immune cell infiltration observed in OLP lesions, and estrogen would regulate gingival epithelial homeostasis (Fig. 13).

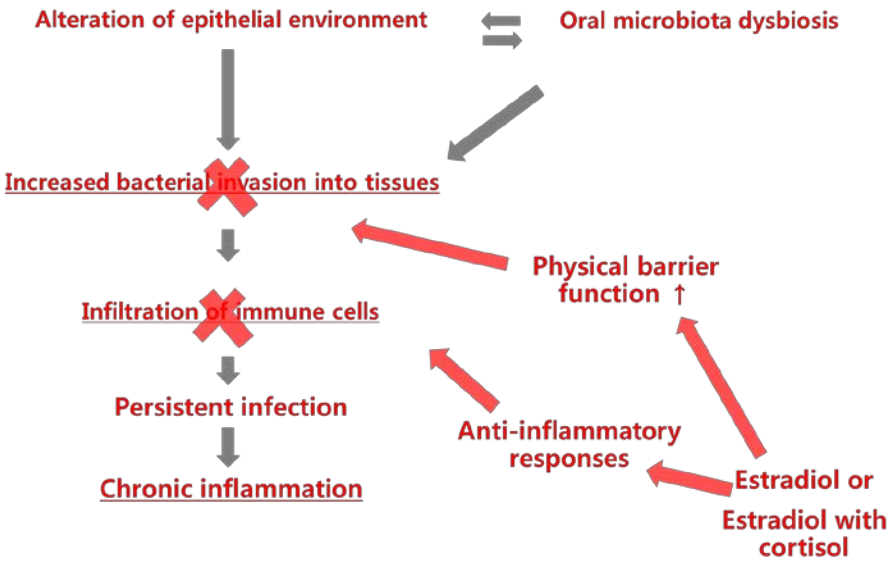

Figure 13. Hypothesis for the present study. Bacterial invasion into the mucosal tissue may be the cause of immune cell infiltration in OLP tissues and estrogen would regulate gingival epithelial homeostasis.

Under the hypothesis of the present study, six questions were addressed. First, bacterial invasion within mucosal tissues was determined. Second, the correlation between bacterial invasion and immune cell infiltration was investigated. Third, bacterial composition was characterized in OLP patients and healthy subjects. Fourth, the internalization and survival of oral bacteria within immune cells was studied. Fifth, the effects of 17β-estradiol on the epithelial physical barrier were investigated. Sixth, the anti-inflammatory responses of 17β-estradiol on the gingival epithelial cells were investigated.

Chapter II. Materials and Methods

2.1. Study population and sample collection

This study was performed according to the Declaration of Helsinki and conformed to the STROBE guidelines. The protocol was approved by the institutional review board at the Seoul National University Dental Hospital (SNUDH) (CRI 12032). Sixteen patients diagnosed with OLP at the Oral Medicine Clinic, SNUDH in 2013 were enrolled, and an Informed Consent was obtained from all subjects. All enrolled patients had no history of antibiotics or steroid treatment within the last month, and had > 0.1 ml/min unstimulated whole salivary flow rate. Smokers were excluded. REU scoring system was adapted to examine the objective sign. It represented the reticulation/keratosis (R), erythema (E) and ulceration (U) of the lesions and it also correlated well with the pain of patients (Park et al., 2012). The numerical rating scale (NRS) was used for the subjective pain of patients (Park et al., 2012). For the mucosa sampling, a sterilized 20 mm x 20 mm polyvinylidene difluorid membrane was placed on the left or right buccal mucosa of subjects for 30 seconds. A punch biopsy was performed on the lesion with reticulation/keratosis. On histopathologic examination, 3 cases diagnosed with candidiasis or chronic mucositis were excluded, and 13 cases diagnosed with OLP or OLL were included for the study.

Additional tissue sections of 23 OLP cases and 10 normal oral mucosa were obtained from the tissue bank at the Department of Oral Pathology, SNUDH, after approval by the IRB at the SNUDH (CRI12023). In total, 36 OLP cases were reviewed again by an oral pathologist and scored for each histopathologic feature of OLP and OLL (Thornhill et al., 2006).

2.2. *In situ* hybridization

A 70-bp DNA fragment 5'-CAGGTGCTGCATGGCTGTCGTCAGCTCGTGTTGTGAAATGTTGG GTTAAGTCCCGCAACGAGCGCAACCC-3') chosen for the well conserved area located between V6 and V7 of *Escherichia coli* 16S rRNA was synthesized as an oligonucleotide and amplified by PCR using the following primers: 5'-CAG GTR CTG CMT GGY-3' and 5'-AGG GTT GCG CTC GTT-3'. Amplifications were performed with following cycling conditions. 40 cycles at 94°C for 30 sec, 60 °C for 30 sec and 72 °C for 1 min 20 s followed by a 5 min extension at 72 °C. After purification, amplified products were labeled with digoxigenin (DIG)-dUTP by random priming using a DIG DNA labeling and detection kit (Roche Applied Science, Penzberg, Germany) to produce DIG-labeled probes.

Serial paraffin-embedded sections (4 μm) were subjected to de-paraffinization, re-hydration, and sequential pre-treatment with 0.1N HCl, 1 μg/ml proteinase K, and 0.1 M triethanolamine-HCl. The DIG-labeled probes were diluted in a hybridization buffer (4x SSC, 50% formamide, 1x Denhardt's solution, 10% dextran sulfate, 0.1% sodium dodecyl sulfate, 0.4 mg/ml salmon sperm DNA), heated at 100 °C, and chilled on ice. After the probe was applied onto tissue sections, the slides were incubated at 90 °C and hybridized in humidified chamber overnight at 45 °C. As a negative control, hybridization was performed with the labeled probe with a 10-fold excess amount of non-labeled probe. After washing with serial SSC, the tissue sections were blocked and hybridized probes were detected with anti-DIG antibody conjugated alkaline phosphatase (Roche Applied Science). The tissues sections were treated with levamisole (Vector Laboratory, Burlingame, CA, USA) to inactivate endogenous alkaline phosphatase and visualized with premixed nitroblue tetrazolium/ 5-bromo-4-chloro-3-indolyl phosphate (NBT-BCIP) solution (Roche Applied Science). The tissue sections were then applied with methyl green as counter stain and mounted.

2.3. Immunohistochemistry

Following de-paraffinization, re-hydration, heat-induced antigen retrieval with citrate buffer, quenching of endogenous peroxidase with Dual endogenous peroxide block (DAKO, Santa Barbara, CA, USA), and the tissues sections were blocked with 5% bovine serum albumin (BSA). The tissue sections were then incubated with anti-CD4 antibody clone 4B12 (Monosan, Sanbio, Uden, the Netherlands), anti-CD8 antibody clone 4B11 (Serotec, Blackthorn, Bicester, England), and anti-macrophage-specific antibody clone 3A5 (Serotec). The bounded primary antibodies were detected using DAKO Envision™ + Dual Link System-HRP kit (DAKO). The visualized sections were then counterstained with hematoxylin (DAKO), dehydrated, and mounted.

2.4. Dual detection of bacterial signals and CD8 markers

For dual detection of bacterial signals and CD8 markers, the tissue sections were subjected to *in situ* hybridization of 16S rRNA first. After quenching of endogenous peroxidase with Dual endogenous peroxide block, the tissues sections were blocked with 5% BSA. After incubation of anti-CD8 monoclonal antibody for 1 h, the bounded antibodies were detected using DAKO Envision TM + Dual Link System-HRP kit. The visualized sections were then counterstained with methyl green, dehydrated, and mounted.

2.5. Image analyses

The signals of *in situ* hybridization and immunohistochemistry were quantified using imageJ software (National Institute of Mental Healath, Bethesda, MD, USA). The tissues section were photographed at x 200 or x 400 magnification. After defining the region of interest (ROI), the positive signals of 3,3´-diaminobenzidine (DAB) or NBT-BCIP from original images were separated using color deconvolutions (Ruifrok and Johnston, 2001). The mean intensity of signals was then evaluated.

2.6. Pyrosequencing

Genomic DNA of mucosal samples was isolated from the polyvinylidene difluorid membranes using the PowerSoil DNA Isolation Kit (MO BIO Laboratories, Carlsbad, CA, USA). 31 mucosa samples (n=18 and n=13 for healthy subjects and patients with OLP or OLL, respectively) were subjected to pyrosequencing analysis. The amplication and sequencing of 16S rRNA genes were performed at ChunLab Inc. (Seoul, Korea) according to the previously described method (Chun et al., 2010) using a 454 GS FLX Titanum Sequencing System (Roche, Branford, CT, USA).

The basic analysis was performed following the previous description

(Chun et al., 2010). After elimination of PCR primer sequences, any reads including two or more ambiguous nucleotides or reads shorter than 300 bp were removed. Chimera sequences were detected by bellerophone method (Huber et al., 2004) and then were also removed. To classify the taxonomy, each read was assigned against EzTaxon database-e (http://eztaxon-e.ezbiocloud.net) (Chun et al., 2007), which includes phylotypes of both cultured and uncultured entries in the GenBank database with complete hierarchical taxonomic classification from the phylum to the species. To calculate the spcies richness and diversity index, Ribosomal RNA database project's pyrosequencing pipeline (http://pyro.cme.msu.edu/) was used. 97% similarity was the cutoff value for for assigning a sequence to the same phylotype. To equalize read size of samples for comparing different read sizes among samples, random subsampling was performed. The overall phylogenetic distance between communities was determined using weighted Fast UniFrac (Hamady et al., 2010) and represented graphically using principal coordinate analysis (PCoA).

2.7. Bacterial culture

Selected bacteria used in this study were from ATCC (American type culture collection) and KCOM (Korean Collection for Oral Microbiology).

Streptococcus sanguinis ATCC 804 and *S. gordonii* ATCC 10558 were cultured in brain heart infusion (BHI) medium at 37 °C under aerobic condition. *C. gingivalis* KCOM 1581 was cultured in BHI medium supplemented with 5 μg/ml of hemin (Sigma, St Louis, MO, USA) plus 10 μg /ml vitamin K under anaerobic condition (5% H_2, 10% CO_2, and 85% N_2). Bacteria in the log phase were obtained and washed three times with phosphate buffer saline (PBS). For application of florescence, bacteria were stained with 5-(and 6-) carboxy-fluorescein diacetate succinimidyl ester (CFSE; Molecular probes, Eugene, OR, USA).

2.8. Human epithelial cell culture

The immortalized human oral keratinocytes (HOK-16B) cells originated from retromolar gingival tissues were maintained in keratinocyte growth medium (KGM) supplemented with supplementary growth factor bullet kit (Clonetics, Sandiego, CA, USA) in an atmosphere with 5% CO_2 at 37 °C. Cells were subcultured at 70-80% confluence.

2.9. Measurement of trans-epithelial electronical resistance after bacterial infection

HOK-16B cells were detached from 100 mm dish by trypsin-EDTA (Gibco, Carlsbad, CA, USA) and washed with pre-warmed KGM medium. The cells (1.0 x 105 cells) were plated onto a 3μm-pore-size polycarbonate filter of a 24-well plate of the transwell two-chamber tissue culture system (SPL life science, Korea). Transepithelial electrical resistance (TER) was assessed using an ERS Volt-Ohm Meter (Millipore Bedford, MA USA). A resistance of epithelial layer > 10 Ω was considered to imply a tight-junctioned epithelial layer (Lux et al., 2001). The cells were cultured for 2 or 3 days with daily medium change until a confluent monolayer reached the peak resistance of about 15 Ω, and then infected with *S. sanguini*, *S. gordonii*, and *C. gingivalis* at the multiplicity of infection (MOI) of 500. TER was measured at 0, 6, 12, and 24 h.

For the assay of cell viability, HOK-16B cells (1.0 x 10^5 cells) were plated. After formation of confluent monolayer, the cells were infected with *S. sanguinis, S. gordonii,* and *C. gingivalis* at MOI 500 for 24 hours. Next, 20 μl of CCK-8 solution (Dojindo, Kumamoto, Japan) was applied to each well. The cells were further incubated for 1 h, and then absorbance was measured at 450 nm using a VERSAmax Tunable microplate reader (Molecular devices, Sunnyvale, CA MA, USA). The cell viability was calculated as a relative percentage of vehicle control.

2.10. Purification of primary human $CD4^+$, $CD8^+$, and $CD14^+$ cells

Peripheral blood purchased from the Red Cross was used and the use of human material was approved by the IRB at Seoul National University, School of Dentistry (IRB No.S-D20150007). Peripheral blood diluted in Dulbecco's phosphate buffer saline (DPBS) at 1:1 was layered on Ficoll-Hypaque (Amersham biosciences, Uppsala, Sweden) at 720g for 30 min. Buffy coat layer containing lymphocytes and monocytes was separated and washed three times with complete RPMI medium (10% heat inactivated FBS, 2 mM L-glutamine, 25 μM 2-mercaptoethanol, and 100 U/ ml penicillin/streptomycin). Peripheral blood mononuclear cells (PBMCs) were re-suspended in RPMI complete medium. To purify $CD14^+$ cells, isolated human PBMCs were incubated with anti-human CD14 magnetic particles on the BD IMagnet™ (BD) for 30 min. After removing the medium containing negative fraction, CD14 positive fractions are collected and re-suspended in the fresh RPMI medium. To purify $CD4^+$ and $CD8^+$ cells, $CD14^+$ cells-depleted PBMC were further incubated with anti-human CD4 magnetic particles (BD) and anti-human CD8 magnetic particles (BD) for 30 min on the BD IMagnet™. After removing the medium containing negative fraction, positive fractions for each cell are collected and re-suspended in the fresh

RPMI medium. After washing three times with RPMI without antibiotics, the cells were plated.

2.11. Bacterial internalization into human cells

HOK-16B cells plated at a density of 3 x 10^4 cells cm^{-2} onto 24-mm diameter glass cover slips (Fisher Scientific, Houston, TX) were infected at 70% confluence with the CFSE-labeled bacteria at MOI 1000 for 4 h. Purified human $CD4^+$, $CD8^+$, or $CD14^+$ cells (2.5 x 10^5 cells) in RPMI medium with 10% FBS were infected with the CFSE-labeled bacteria at MOI 1000 without antibiotics for 1 h. After fixation with 4% paraformaldehyde (PFA) for 30 min and permiabilization with 0.3% PBST for 10 min, the infected cells were stained with rhodamine-phalloidin (Molecular probes) and Hochest 33342 (Molecular probes) for 30 min. After washing with distilled water, the leukocytes were attached onto collagen-coated slides. Mounted slides were imaged using a Zeiss LSM700 (Carl Zeiss, Oberkochen, Germany) with serial z-sections.

For flow cytometric analysis, the infected cells were washed with PBS and resuspended in trypan blue (400 mg ml^{-1} prepared in 0.85% saline solution) to quench the fluorescence of the bacteria bound on the surface. The cells were analyzed using a FACSCalibur (BD biosciences). The cells were

gated first on the appropriate population based on the forward vs. side scatters and then on the live cells based on the FL-3 fluorescence of trypan blue. The cells were fixed with 3.7% formaldehyde and infected with the same MOI of CFSE-labeled bacteria served as a negative control.

2.12. Antibiotics protection assay

To examine the persistence of intracellular bacteria, purified human $CD4^+$, $CD8^+$, or $CD14^+$ cells (5.0×10^5 cells) were infected with selected bacterial species at MOI 1000 for 1 and 24h in the presence of gentamycin (50 μg ml^{-1}). The infected cells were washed with PBS and lysed with sterile distilled water containing 0.5% saponin. After washing with PBS, the lysates were plated onto blood agar plate with hemin and vitamin K under an appropriate atmosphere for 2-3 days.

2.13. Cytokine ELISA and multiplex assay

The levels of chemokines in the culture supernatant of HOK-16B, $CD4^+$, $CD8^+$, and $CD14^+$ cells were measured by ELISA and multiplex assay. HOK-16B, CD4+, CD8+, and CD14+ cells were infected with the three bacterial species for 1 h and further cultured in the presence of gentamycin

(50 μg ml^{-1}) for 23 h. The culture supernatant of infected cells and non-infected control cells was obtained and stored at -80 °C until use. The amounts of CXCL8 (IL-8) secreted into the medium during infection with selected bacteria were measured using ELISA kit (R&D systems, Minneapolis, MN, USA) following manufacture's introduction. The amounts of CCL3 (MIP-1α), CCL5 (RANTES), and CXCL10 (IP-10) were determined using Multiplex assay kit (R&D systems) according to manufacture's instruction.

2.14. Measurement of TER under the normal condition

To investigate the effect of 17β-estradiol on the gingival epithelial barrier in the normal condition, HOK-16B cells (4.0×10^4 cells) were plated onto a 3μm-pore-size polycarbonate filter of a 24-well plate of the transwell two-chamber tissue culture system one day before 17β-estradiol treatment. The cells were treated with 0.2, 2, or 2 nM 17β-estradiol treatment. TER was measured using an ERS Volt-Ohm Meter at 6, 12, 24, 48, 72, and 96 h.

2.15. Measurement of TER under the pro-inflammatory cytokine-induced damaged condition

To examine the effect of TNF-α on the gingival epithelial barrier, HOK-16B cells were cultured for 2 or 3 days with daily medium change until a confluent monolayer reached the peak resistance. Tight-junctioned monolayers of HOK-16B were treated with TNF-α (10-250 ng/ml) (R&D systems) for 24 h. TER was assessed using an ERS Volt-Ohm Meter at 0, 2, 4, 8, and 24 h.

To determine the protective effect of 17β-estradiol on the gingival epithelial barrier under the pro-inflammatory cytokine-induced damaged condition, tight-junctioned monolayers of HOK-16B were pre-treated with either ICI 182,780 (125 μM) (Sigma-Aldrich, St. Louis, MO, USA) for 2 h or 17β-estradiol (2-20 nM) for 4 h. The cells were then treated with TNF-α (100 ng/ml) (R&D systems) for 24 h. TER was measured using an ERS Volt-Ohm Meter at 24 h.

2.16. CCK-8 assay

To investigate the effect of 17β-estradiol on the proliferation of gingival epithelial cells under the normal condition, HOK-16B cells (4×10^4 cells/well) were plated in 96-well plate. The cells were treated with 17β-estradiol for 0, 6, 12, 24, 48, 72, and 96 h.

To examine the effect of 17β-estradiol on the viability of gingival epithelial cells under the pro-inflammatory cytokine-induced damaged condition, tight-junctioned monolayers of HOK-16B were treated with TNF-α (10-250 ng ml^{-1}) for 24 h in the absence or presence of 17β-estradiol (2-20 nM) or ICI 182,780 (125 μM).

After treatment for indicated time point, CCK-8 solution was added. The cells were further incubated for 1 h, and then absorbance was measured at 450 nm using a VERSAmax Tunable microplate reader. The cell viability was calculated as a relative percentage of vehicle control.

2.17. Immunofluorescence staining

To determine the effect of estrogen on the expression levels of ZO-1 and JAM-A under the normal condition, HOK-16B cells were plated at 2×10^5 cells onto 12mm diameter collagen coated cover slips in 24-well plate (Fisher Scientific, Houston, TX, USA).

For the pro-inflammatory cytokine-induced damaged condition, HOK-16B cells (5×10^5 cells) were plated onto 12mm diameter collagen coated cover slips in 24-well plate. Tight-junctioned monolayers of HOK-16B

were incubated with TNF-α (20-100 ng ml^{-1}) for 1 or 24 h in the absence or presence of 17β-estradiol (2-20 nM) or ICI 182,780 (125 μM).

After fixation with 4% paraformaldehyde (PFA), the cells were treated with 50 mM ammonium chloride for 10 min to quench autofluorescence. After permiabilization with 0.3% PBST and blocking with 5% BSA, the cells were incubated with rabbit anti-ZO-1 polyclonal antibody (Invitrogen, Carlsbad, CA, USA), mouse anti-JAM-A antibody clone 2E3-1C8 (Abnova, Taipei, Taiwan), and anti-NF-κB p65 polyclonal antibody (Biolegend, San Diego, CA, USA) overnight at 4°C, and then with Alexa 488 anti-rabbit antibody (Invitrogen) or Alexa 555 anti-mouse antibody (Invitrogen) for 1 h. After washing with PBS, the cells were counterstained with Hochest 33342 and mounted. For each slides, five areas were photographed at 100 x magnification using a Zeiss LSM700 with serial Z-section. Maximum intensity projections were obtained by combining the serial Z-section. The fluorescence intensity of ZO-1 and JAM-A was analyzed using ZEN 2010 (Carl Zeiss) and normalized to the fluorescence intensity of Hochest 33342. For quantification of nuclear translocation of NF-κB, co-localized signals of nucleus and NF-κB p65 were measured using ImageJ software. Experiments were repeated twice.

2.18. Real-time Reverse Transcriptional Polymerase Chain Reaction (RT-PCR)

RNA from HOK-16B cells was obtained using EasyBLUE (iNtRON, Seoul, Korea). Total RNA (2 μg) was subjected to reverse transcription (RT) using oligo dT and the M-MLV Reverese trascrpitae enzyme (Promega, Madison, WI, USA) in a 30 μl reaction mixture at 42°C for 1 h. Real time PCR was performed in a 20 μl reaction including each primer (0.4 μl), SYBR Premix EX Taq (10 μl), ROX II reference dye (0.4 μl), and 2 μl template cDNA. Sequences of each primer are listed in table 1. Amplification was performed using fluorescence thermocycler (Applied Biosystem 7500 Real-time PCR, Foster City, CA, USA) under the following conditions: initial denature at 95 °C for 4 min, followed by 35 cyles of denatureation at 95 °C for 15 s, annealing at 60 °C for 15 s, and elongation at 72 °C for 33 s. The glyceraldehyde 3-phosphate dehydrogenase (GAPDH) was amplified in parallel with gene of interest. Relative copy numbers of TJ proteins in comparison with GAPDH were calculated using $2^{-\triangle Ct}$. Real-time PCR was performed in triplicate for each of cDNA samples.

Table 1. Primer sequences used.

Primer	Orientation	Sequence (5'-3')
GAPDH	Forward	CAGCCTCAAGATCATCAGCA
	Reverse	CCATCCACAGTCTTCTGGGT
ZO-1	Forward	GGTCAAGGTCAAGCTCAT
	Reverse	CTGAGTAAGGCAAATGCAG
JAM-A	Forward	GAACGAGGCATCATCCCTAA
	Reverse	CCAGCTTCTCGAAGAACCAC

2.19. Statistics

Data were analyzed using Mann-Whitney U test to determine the differences between the healthy subjects and patients with OLP in the clinical study. To the differences between control and experimental groups, two-tailed non-paired Student's t-test was performed. One-way ANOVA with Tukey's post hoc was used to assess the difference between groups. Logistic regression analysis was used to examine the possibility of OLP risk by relative abundances of bacterial species in oral mucosa. The associations between two parameters in clinical study were analyzed by Speraman's rank correlation. All analyses were performed using SPSS 12.0 (SPSS Inc, Chicago, IL, USA).

Chapter III. Results

3.1. Study population

For this study, the mucosal bacterial samples and biopsies were obtained from 13 new patients diagnosed as OLP in the Oral Medicine Clinic, SNUDH. Among the 13 cases, 7 cases were diagnosed as OLL by one or two pathologists based on the histopathologic features of OLL (Table. 3 and 4) (Thornhill et al., 2006). The detail clinical information of the 13 patients is summarized in Table 2. Tissue sections of 23 OLP cases, which present the typical histopathologic features of OLP and no ulceration in the epithelium of biopsied tissues, and 10 normal oral mucosa were additionally obtained from the tissue bank at the Department of Oral Pathology, SNUDH. The detail histopathologic characteristics of total 36 cases are summarized in Table 3.

Table 2. Clinical information of OLP patients

No	Age	Sex	REU[a] scoring		Pain score	Duration	Sites	Systemic disease with medication	Pathologist 1	Pathologist 2
			REU	Score						
OLP2	67	M	R1E2	4	2	1 year	Buccal mucosa	Hypertension	OLL	OLL
OLP3	59	F	R5E5U1	13.5	8	5 month	Buccal mucosa, Gingiva, Tongue	None	OLP	OLP
OLP5	69	F	R1E2U1	6	4	2 month	Buccal mucosa	Hypertension	OLP	OLL
OLP6	41	F	R2E2U2	9	5	6 month	Buccal mucosa	None	OLP	OLP
OLP8	65	F	R2E2U1	8	4	3 month	Buccal mucosa, Lip, Gingiva	None	OLL	OLL
OLP9	50	F	R3E8U2	19	5	6 month	Buccal mucosa, Gingiva	None	OLL	OLL
OLP10	29	M	R1E1	2.5	4	3 month	Buccal mucosa	Manic depression	OLP	OLL
OLP12	70	M	R1E2U1	6	5	6 month	Buccal mucosa	Hypertension, Diabetes	OLP	OLP
OLP13	53	M	R3E1	4.5	4	10 month	Buccal mucosa, Tongue, Palate	None	OLL	OLL
OLP14	56	M	R3E2U1	3.5	4	3 month	Buccal mucosa, Palate	Hypertension, Paresthesia	OLP	OLP
OLP15	56	M	R1E2	4	4	1 month	Buccal mucosa	None	OLP	OLP
OLP16	58	M	R4E9U4	25.5	7	4 year	Buccal mucosa, Gingiva, Tongue	Colon cancer	OLP	OLL
OLP19	66	F	R5E8	17	4	6 month	Buccal mucosa, Gingiva, Palate	None	OLP	OLP

[a]R, reticulation/keratosis; E, erythema; U, ulceration

Table 3. The detail histopathologic characteristics of total 36 cases

Patients	1	2	3	4	5	6	7	8	9	10	11	12	13	14	15	16	17	18	19	20	21	22	23	24	25	26	27	28	29	30	31	32	33	34	35	36	37
OLP2	0	1	1	1	0	0	0	0	0	0	1	0	0	0	1	0	1	1	0	1	0	1	1	-1	-1	0	1	1	-1	0	0	1	0	0	0	1	1
OLP3	0	1	1	0	0	0	0	0	0	0	1	0	0	0	1	0	1	1	0	1	0	0	1	0	0	1	0	1	-1	-1	0	1	1	0	0	1	1
OLP5	0	1	0	1	0	0	0	0	0	1	1	0	0	0	0	0	1	0	0	0	-1	1	1	-1	-1	0	1	1	-1	-1	0	0	0	0	0	1	1
OLP6	0	1	0	0	1	0	0	1	0	0	1	0	1	0	0	0	1	0	1	0	0	0	1	0	0	1	0	1	-1	0	0	0	0	0	1	0	1
OLP8	0	1	0	0	1	0	0	1	0	0	1	0	0	0	0	0	1	1	0	1	0	0	1	-1	0	0	1	1	-1	0	0	1	0	0	1	1	1
OLP9	0	1	0	1	0	0	1	0	0	0	1	0	0	0	0	0	1	1	0	1	0	0	1	-1	-1	0	1	1	-1	0	0	0	0	0	1	1	0
OLP10	0	1	0	0	1	0	0	1	0	1	1	0	0	0	0	0	1	1	0	1	0	0	1	0	0	1	0	1	-1	-1	-1	0	0	1	1	1	1
OLP12	0	1	0	0	1	0	0	1	0	0	1	0	1	1	0	0	1	0	1	0	0	0	1	0	0	1	0	1	0	-1	0	1	0	1	0	1	1
OLP13	0	1	0	0	1	0	0	0	0	1	1	0	0	0	0	0	0	1	0	1	0	1	1	-1	-1	0	1	1	-1	0	0	0	0	1	1	1	1
OLP14	0	1	0	0	0	1	0	1	0	0	1	0	0	1	0	0	1	0	1	0	0	0	1	0	0	1	0	1	0	0	-1	1	0	0	1	1	1
OLP15	0	1	0	0	1	0	0	1	0	0	1	0	0	0	0	0	1	0	1	0	0	0	1	0	0	1	0	1	-1	0	-1	0	0	1	1	1	0
OLP16	0	1	0	1	0	0	1	0	0	0	1	0	0	0	0	0	1	0	0	0	-1	0	1	-1	-1	0	1	1	-1	0	-1	1	0	1	1	0	0
OLP19	0	1	0	0	1	0	0	1	0	0	1	0	0	0	0	0	0	0	1	0	0	0	1	0	0	1	0	1	0	0	0	1	0	1	0	1	0
OLP20	1	1	0	1	0	0	0	1	1	0	1	0	1	0	0	0	0	1	0	1	0	0	1	0	0	1	0	1	0	0	0	1	1	0	0	1	0
OLP21	0	1	0	0	0	0	0	1	0	0	1	1	0	0	0	0	1	0	1	0	0	0	1	0	0	1	0	1	0	0	0	0	0	0	0	0	0
OLP22	0	1	0	0	0	1	0	1	0	0	1	0	1	0	1	0	0	0	1	0	0	0	1	0	0	1	0	1	0	0	0	1	0	0	0	0	0
OLP23	0	1	1	1	0	1	0	1	0	0	1	0	0	0	0	0	1	0	1	0	0	0	1	0	0	1	0	1	-1	0	1	0	0	0	0	0	0
OLP24	0	1	0	1	0	0	1	0	0	0	1	0	1	0	0	0	0	0	1	0	0	0	1	0	0	1	0	1	0	0	0	1	0	1	0	0	0
OLP25	0	1	0	1	0	0	0	1	0	0	1	0	0	0	0	0	0	0	1	0	0	0	1	0	0	1	0	1	0	0	0	0	0	1	0	0	0
OLP26	0	1	1	0	0	0	0	0	0	0	1	1	0	0	0	0	0	0	1	0	0	0	1	0	0	1	0	1	0	0	0	1	0	0	0	1	1
OLP27	0	1	0	1	0	0	0	1	0	0	1	1	1	0	0	0	1	0	1	0	0	0	1	0	0	1	0	1	0	0	0	0	0	1	0	1	1
OLP28	0	1	0	1	0	0	0	1	0	0	1	0	0	0	0	0	1	0	1	0	0	0	1	0	0	1	0	1	0	0	0	0	0	0	0	1	1
OLP29	0	1	0	1	0	0	0	1	1	0	1	0	0	0	0	0	0	0	1	0	0	0	1	0	0	1	0	1	0	0	0	1	0	0	0	0	1
OLP30	0	1	0	1	0	1	0	1	1	0	1	0	1	0	0	0	0	1	0	1	0	0	1	0	0	1	0	1	0	0	0	1	0	0	0	0	0
OLP31	0	1	0	1	0	0	0	1	0	0	1	0	1	0	0	0	0	1	0	0	0	0	1	0	0	1	0	1	0	0	0	1	0	0	0	0	1
OLP32	0	1	0	0	0	1	1	1	0	0	1	0	0	0	0	0	0	0	1	0	0	0	1	0	0	1	0	1	0	0	0	1	0	1	0	0	0
OLP33	0	1	0	0	0	1	0	1	0	0	1	0	0	0	0	0	0	0	1	0	0	0	1	0	0	1	0	1	0	0	0	1	0	1	0	0	1
OLP34	0	1	0	0	1	0	0	1	0	0	1	0	0	0	0	0	0	0	1	0	0	0	1	0	0	1	0	1	0	0	0	0	0	0	0	0	1
OLP35	0	1	1	0	0	1	0	0	0	0	1	0	1	0	0	0	0	0	1	0	0	0	1	0	0	1	0	1	0	0	0	1	1	1	0	0	0
OLP36	0	1	0	1	0	0	0	1	0	0	1	0	0	0	0	0	1	0	1	0	0	0	1	0	0	1	0	1	-1	0	0	0	0	0	0	0	1
OLP37	0	1	1	0	0	0	0	0	0	0	1	1	0	0	0	0	0	1	0	1	0	0	1	0	0	1	0	1	0	0	0	1	0	0	0	0	1
OLP38	0	1	1	0	0	0	0	0	0	0	1	0	0	0	0	0	1	0	1	0	0	0	1	0	0	1	0	1	0	0	0	1	1	1	0	0	1
OLP39	0	1	0	1	0	0	0	1	0	0	1	0	0	0	0	0	1	0	1	0	0	0	1	0	0	1	0	1	0	0	0	1	0	1	0	0	1
OLP40	0	1	0	0	0	1	0	0	0	0	1	0	0	0	0	0	1	0	1	0	0	0	1	0	0	1	0	1	0	0	0	1	0	1	0	0	1
OLP41	0	1	0	0	0	1	0	1	0	0	1	0	1	0	0	0	1	0	1	0	0	1	1	0	0	1	0	1	0	0	0	1	0	0	0	0	1
OLP42	0	1	1	0	0	0	0	0	0	0	1	1	0	0	0	0	0	0	1	0	0	0	1	0	0	1	0	1	0	0	0	1	0	0	0	0	0

Table 4. List of histological features adapted from Schiødt (Thornhill et al., 2006)

Histological features
Epithelium – keratinization
1. Hyperorthokeratosis
2. Hyperparakeratosis
Epithelium – thickness and configuration
3. Atrophy; reduction in thickness more than 1/3 of normal area
4. Acanthosis; broadening of rete ridges more than two time normal width for area
5. Simple hyperplasia; thickness more than 1 1/2 time normal thickness for area, excluding stratum corneum
6. Atrophy alternating with hyperplasia
7. Finger-like rete ridges
8. Sawtooth rete ridges *Fusobacterium nucleatum*
Epithelium – other
9. Thick stratum granulosum, more than five cell layers thick
10. Migration by leucocytes; easily visible small groups or heavy infiltration by leucocytes
11. Liquefaction degeneration of basal layer
12. Intraepithelial vesicles; subepithelial vesicles excluded epithelial cellular

changes

13. Colloid bodies – civatte bodies

14. Multinucleated epithelial cells; cells containing three or more nuclei

15. Hyperchromatism

16. Epithelial dysplasia; slight, moderate or severe

17. Supra-basilar apoptosisa (connective tissue – superficial inflammatory infiltrate)

18. Band-shaped infiltrate, some areas

19. Band-shaped infiltrate, all areas

20. Not band-shaped infiltrate, some areas

21. Not band-shaped infiltrate, all areas

22. Focal/perivascular infiltrate

23. Intensity of inflammatory infiltrate: moderate or heavy (connective tissue – deep inflammatory infiltrate)

Connective tissue – deep inflammatory infiltrate

24. Deep inflammatory infiltrate; located deep to superficial infiltrate, some or all areas

25. Focal/perivascular infiltrate

26. Intensity of inflammatory infiltrate: none

27. Intensity of inflammatory infiltrate: slight

Connective tissue – cell types of inflammatory infiltrate

28. Lymphocytes and histiocytes

29. Plasma cells

30. Neutrophils

31. Eosinophils

Connective tissue – juxtaepithelial area

32. Juxtaepithelial cell-free zone; narrow eosinophilic zone separating (basal cells from inflammatory infiltrate)

33. Hyalinization of collagen

34. Melanophages

35. Oedema

Connective tissue – vessels

36. Dilatation of vessels

37. Neutrophils in lumen of vessels

3.2. Increased bacterial invasion in OLP lesions

3.2.1. Increased bacterial invasion into lamina propria in OLP patients

To determine bacterial invasion of mucosal tissue in OLP lesions, *in situ* hybridization was performed using a digoxigenin (DIG)-labeled eubacterial probe targeting bacterial 16S rRNA. In the control oral mucosa, the bacterial signals were often detected within the epithelia but rarely in the lamina propria (Fig. 14a). However, strong bacterial signals were detected in the lamina propria of all OLP tissues (Fig. 14b). Accordingly, the intensity of the bacterial signals in the lamina propria was significantly higher in the OLP than the control tissues, while that in the epithelia was not different (Fig. 14c).

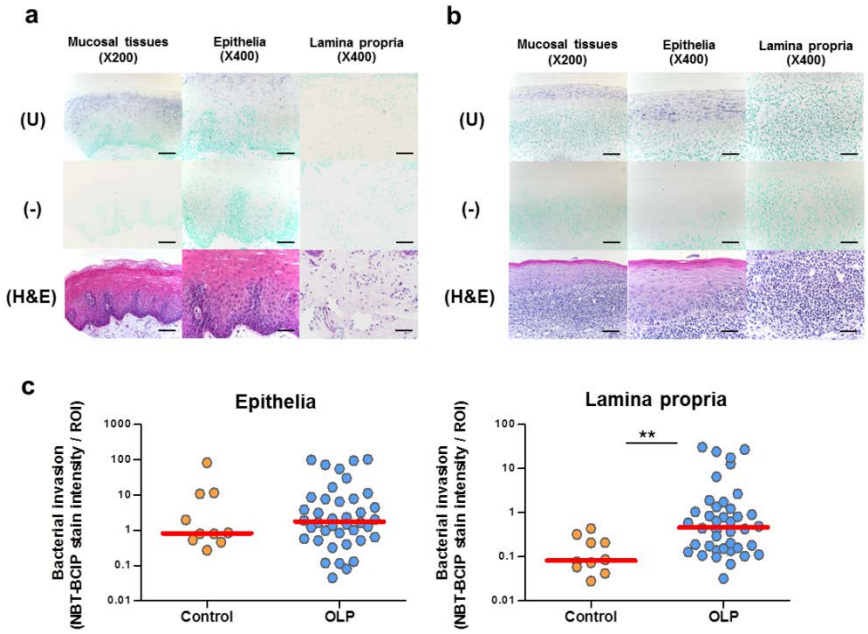

Figure 14. Increased bacterial invasion into lamina propria in OLP patients. a-b) Representative *in situ* detection of bacteria in the control (n = 10) and OLP tissues (n = 36). Mucosal tissues from control subjects **(a)** and OLP patients **(b)** stained with hematoxylin and eosin or were *in situ* hybridized with a digoxigenin (DIG)-labeled eubacterial probe targeting bacterial 16S rRNA (U). As a negative control (-), *in situ* hybridization was performed using a probe mixed with 10-fold excess of unlabeled probe. The mucosal epithelia and lamina propria were photographed (scale bar = 100 μm and 50 μm, 200 x and 400 x, respectively). Violet colors indicate positive signals. **c)** The mean intensity of stained signals per ROI in the epithelia and

lamina propria was analyzed using ImageJ software and is expressed as the median of each group. **, $P < 0.01$ (Mann-Whitney U test).

3.2.2. A strong positive correlation between the levels of bacteria within lamina propria and those within the epithelia in the OLP tissues

Although the total amount of bacteria detected within the epithelia was not different, the incidence of bacterial detection within the basal layer of the epithelia was significantly different (10.0% vs 72.5%), indicating it as the risk factor for OLP (odds ratio [OR] 23.7, 95% confidence interval [95% CI] 2.7-209.8, $P = 0.004$) (Fig. 15). In addition, the levels of bacteria detected within the lamina propria had a strong positive correlation with those within the epithelia in the OLP ($r = 0.651$, $P < 0.001$), but not in the control tissues ($r = 0.149$, $P = 0.371$, Fig. 16). Collectively, these results indicate that the bacterial invasion into the lamina propria is increased in OLP tissues, which agrees with liquefaction of the basal layer.

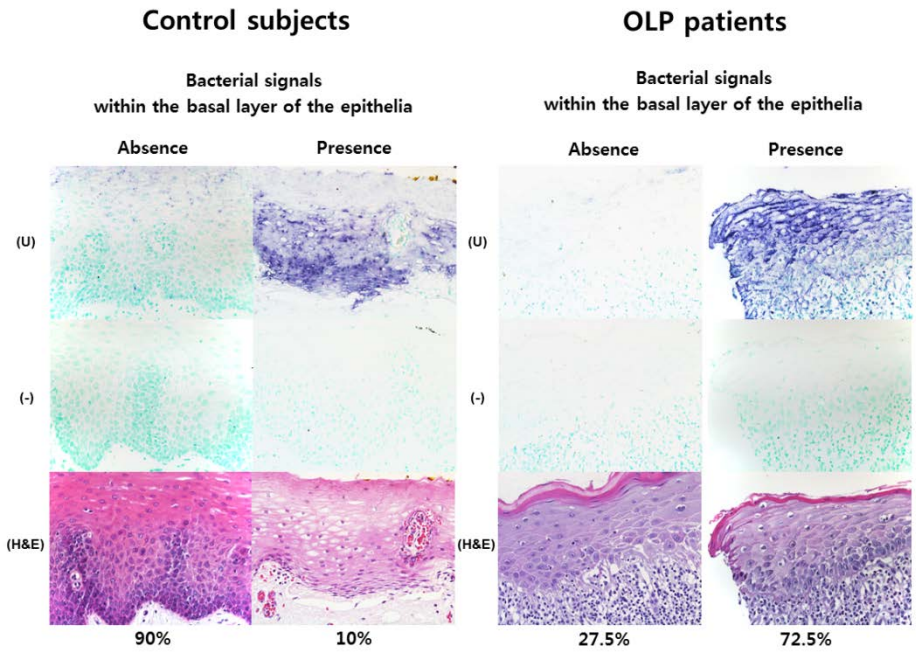

Figure 15. Different pattern of bacterial detection within epithelia between control subjects and OLP patients. Representative *in situ* detection of bacteria in the control (n = 10) and OLP tissues (n = 36). The mucosal tissues from control subjects and OLP patients stained with hematoxylin and eosin or were *in situ* hybridized with DIG-labeled eubacterial probe targeting bacterial 16S rRNA (U). As a negative control (-), *in situ* hybridization was performed using a probe mixed with 10-fold excess of unlabeled probe. The mucosal epithelia were photographed (scale bar = 100 μm, 400 x). Violet colors indicate positive signals.

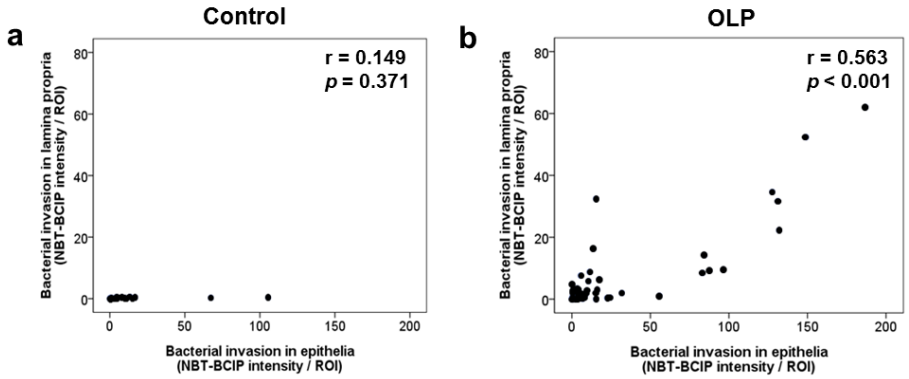

Figure 16. A strong positive correlation between the levels of bacteria within lamina propria and those within the epithelia in the OLP tissues. The mucosal epithelia and lamina propria were photographed (400 x). The mean intensity of stained signals per ROI in the epithelia and lamina propria was analyzed using ImageJ software. **a-b)** Two-tailed Spearman's rank correlations between the levels of bacteria detected within the lamina propria and epithelia are shown.

3.3. Bacteria detected within $CD4^+$ and $CD8^+$ T cells

As one of the well-known features, all OLP tissues presented band-like infiltration of lymphocytes that were mostly $CD4^+$ and $CD8^+$ T cells (Fig. 17a-c). Interestingly, bacteria were often detected within the nuclei of inflammatory cells of lymphocyte morphology (Fig. 17d). Dual detection of bacterial signals and CD8 revealed the presence of bacteria within the $CD8^+$ T cells. Although dual detection of bacterial signals and CD4 was not performed due to non-specific staining of CD4 in the dual staining, the bacterial signals were also observed within $CD8^-$ lymphocytes, presumably $CD4^+$ T cells (Fig. 17e-f). These results suggest that certain oral bacteria can be internalized into both $CD4^+$ and $CD8^+$ T lymphocytes.

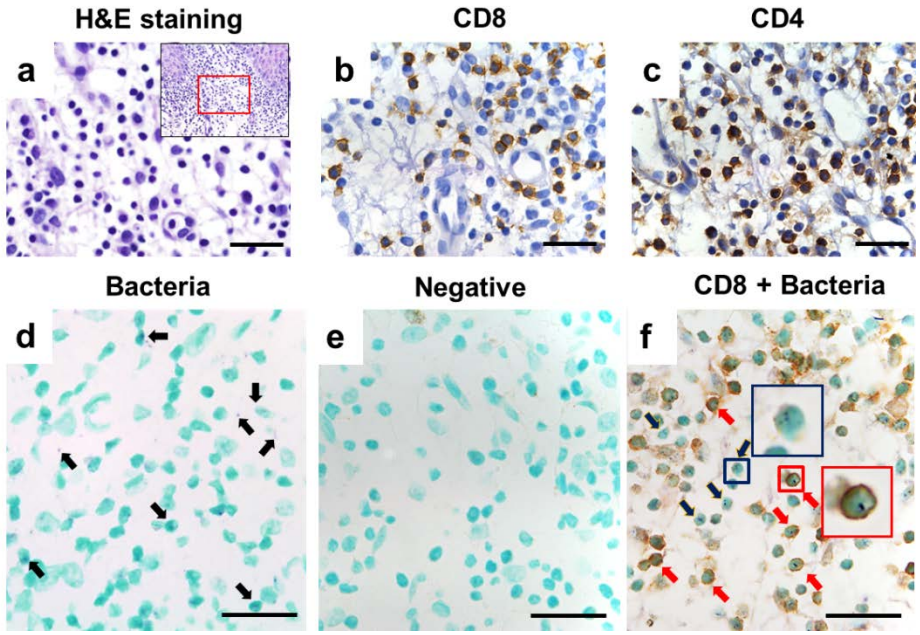

Figure 17. Dual detection of bacterial signals and CD8 marker. a) Mucosal tissues from patients with OLP stained with hematoxylin and eosin. **b-c)** Mucosal tissues from patients with OLP were stained for CD8 **(b)** and CD4 **(a)** by immunohistochemistry. **d)** Mucosal tissues from patients with OLP were *in situ* hybridized with DIG-labeled eubacterial probe targeting bacterial 16S rRNA. The positive signals of bacteria in violet marked with black arrows. **e)** Mucosal tissues were *in situ* hybridized with a negative probe and then stained with an isotype antibody. **f)** Representative dual detection of bacteria in situ and CD8 immunochemistry in OLP tissues (n = 4). Following the *in situ* hybridization protocol, tissues were stained for CD8. Brown colors indicate positive signals of CD8. The bacterial signals within $CD8^-$ cells marked with blue arrows. Bacterial signals within $CD8^+$ cells were indicated

as red arrows. The lamina propria were photographed (scale bar = 25μm, 1000 x).

3.4. A strong positive correlation of the amount of bacteria in the lamina propria with infiltration of $CD4^+$ and $CD8^+$ T cells but not with macrophages

To examine the relationship between bacterial invasion of tissues and immune cell infiltration, the levels of $CD4^+$, $CD8^+$ T cells, and macrophages were determined by immunohistochemistry and quantitated using ImageJ. All three cell types were increased in the OLP compared with the control tissues (Fig. 18a-c). However, only the levels of $CD4^+$ and $CD8^+$ T cell, but not those of macrophages, had a strong positive correlation with the levels of bacteria detected within the lamina propria (Fig. 18d and Fig. 19). These results suggest that bacterial invasion into the lamina propria is strongly associated with infiltration of T cells, key immune cells observed in OLP lesions.

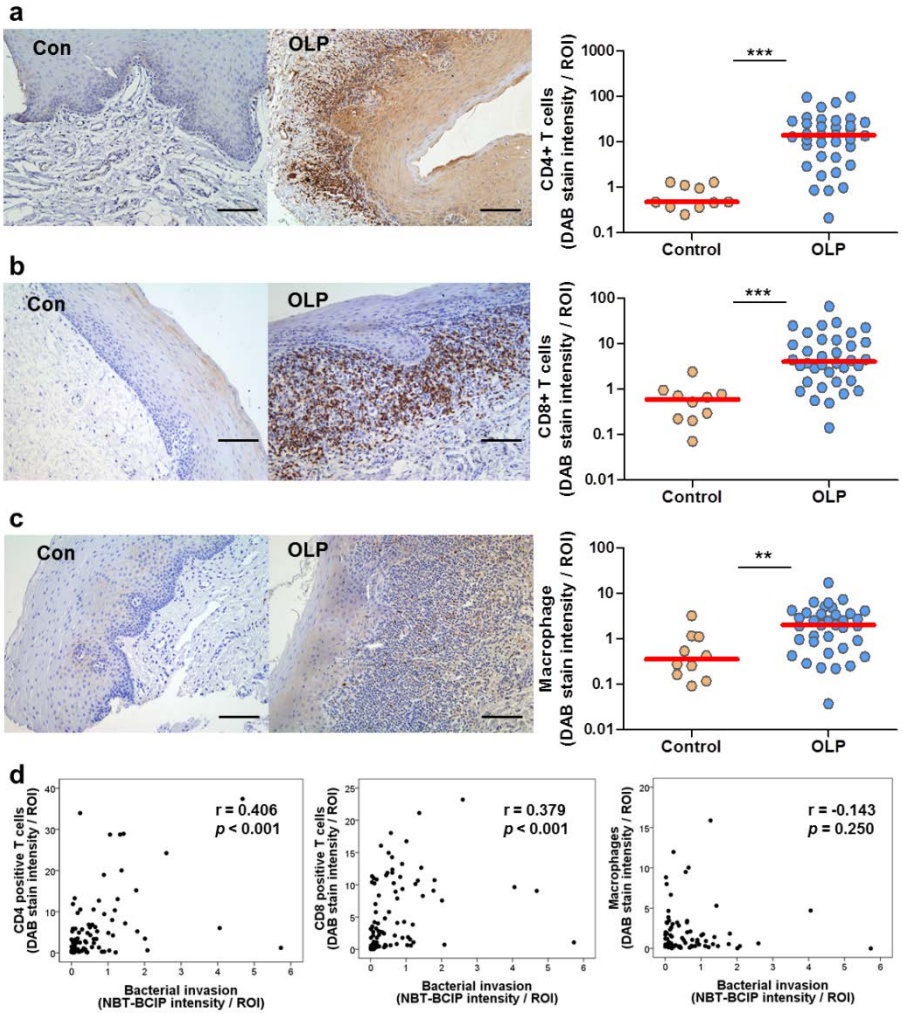

Figure 18. A strong positive correlations of the amount of bacteria in the lamina propria with infiltration of $CD4^+$ and $CD8^+$ T cells but not with macrophages. a-c) Representative results of immunohistochemistry for $CD4^+$ cells **(a)**, $CD8^+$ cells **(b)**, and macrophages **(c)** in control subjects (n = 10) and OLP patients (n = 36). Mucosal tissues from control subject and OLP patients were stained for CD4, CD8, and macrophage by immunohistochemistry. The

entire mucosal samples were photographed (scale bar = 100 μm, 200 x). The mean intensity of stained signals per ROI in the lamina propria was analyzed using ImageJ software and is expressed as the median of each group. **, $P < 0.01$; ***, $P < 0.001$. (Mann-Whitney U test). **d)** Two-tailed Spearman's rank correlation between the levels of bacterial invasion and $CD4^+$, $CD8^+$, or $CD14^+$ cells are shown.

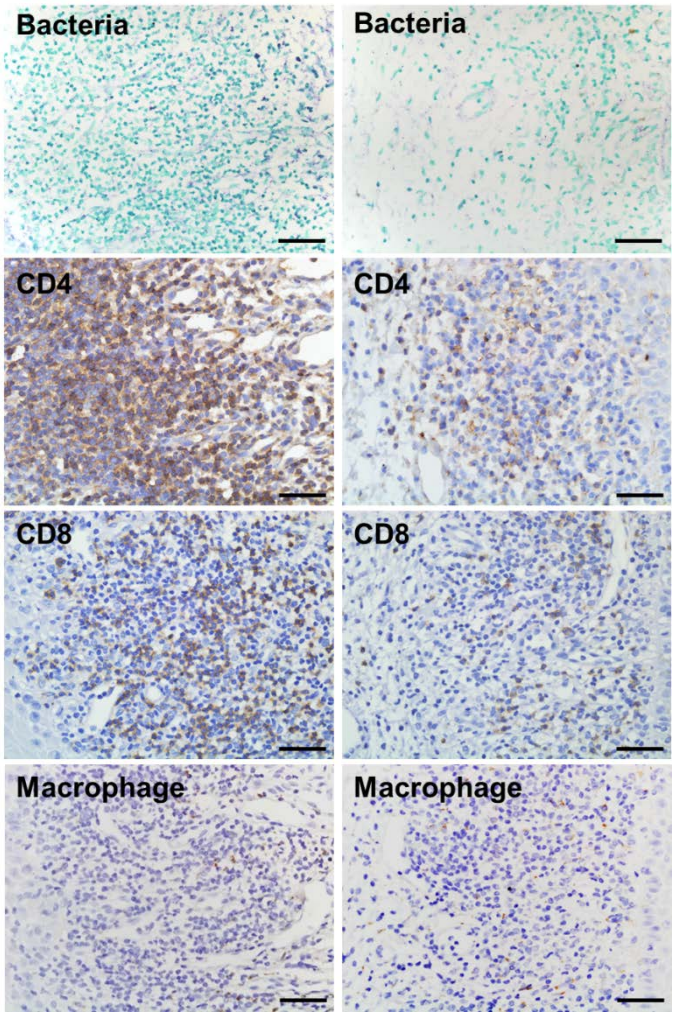

Figure 19. Presence of bacteria in inflamed mucosal tissues. The presence of bacteria in mucosal tissues was detected using an *in situ* hybridization. Mucosal samples from patients with OLP were stained for CD4, CD8, and macrophage by immunohistochemistry. The entire mucosal samples were photographed (scale bar = 100 μm, 200 x). Two areas with different degrees of inflammatory infiltration from a same section are shown.

3.5. Dysbiosis of oral mucosal microbiota in the OLP patients

The bacteria detected within the lamina propria of OLP lesions may be increased on the surface of oral mucosa. To determine changes in the mucosal microbiota of OLP from a healthy state, the bacterial communities collected from the lesion of OLP patients (n=13) were compared with those of healthy control subjects (n=18). The species richness determined by Chao1 (319 ± 19 vs. 361 ± 28, P = 0.293) and microbial diversity determined by Shanon indexes (3.61 ± 0.11 vs. 3.91 ± 0.13, P = 0.068) were tended to increase in the OLP samples (Fig. 20a). In the principal coordinates analysis (PCoA) plot, the clustering of control and OLP samples was not completely separated from each other but presented different distribution (Fig. 20b).

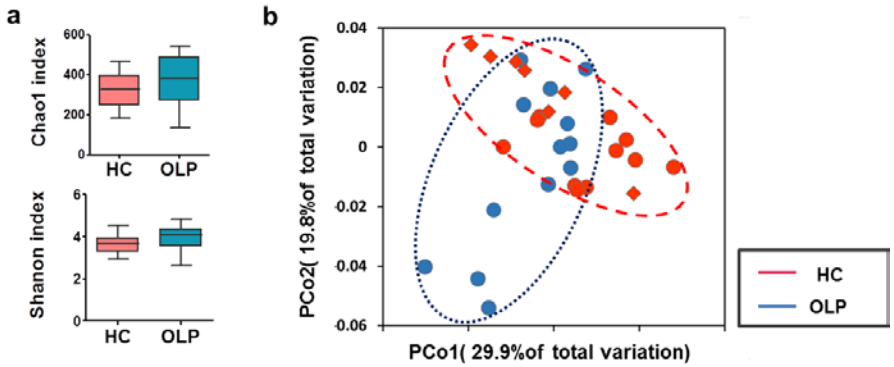

Figure 20. Increased microbial diversity and heterogeneous community in the OLP patients. The bacterial DNA samples obtained from mucosal tissues from healthy subjects (n = 18) and OLP patients (n = 13), and the bacterial community were analyzed using a pyrosequencing of amplified 16S rRNA fragments. **a)** The species richness estimated by Chao1 and Shannon diversity index was expressed as the Box-and-Whisker Plots. **b)** PCoA plot generated using weighted Unifrac metric. (Red circle symbols: control samples of buccal mucosa, red square symbols: control samples of buccal mucosa, and blue circle symbols: control samples).

Comparison of the relative abundance of each taxon revealed many differences in the composition of microbiota between the control and OLP samples. At the phyla level, the relative abundance of Bacteroidetes, Fusobacteria, and Spirochaetes was significantly increased in OLP. At the genus level, the abundance of *Streptococcus* and *Rothia* was decreased, while that of *Prevotella*, *Leptotrichia*, *Capnocytophaga*, *Porphyromonas*, *Aggregatibacter*, *TM7_g*, and *Treponema* was increased in OLP (Fig. 21). Among the 42 species/phylotypes that showed a significant difference in relative abundance between two groups (Table 5), only four species/phylotypes were decreased, while the abundances of 38 species/phylotypes, including *Fusobacterium nucleatum*, *P. gingivalis*, *Neisseria oralis*, *S. gordonii*, *C. gingivalis*, and *Leptotrichia wadei*, were increased in OLP compared to controls. In particular, an increase in the relative abundance (per %) of *C. gingivalis* was associated with OLP risk (OR 2.1E5, CI 95% 2.5-1.8E10, $P = 0.034$). In contrast, a decrease in the relative abundance of *S. sanguinis* (per %) was associated with OLP risk (OR 0.6, CI 95% 0.381-0.955, $P = 0.031$), although the decrease of *S. sanguinis* in the OLP was not significant ($P = 0.157$).

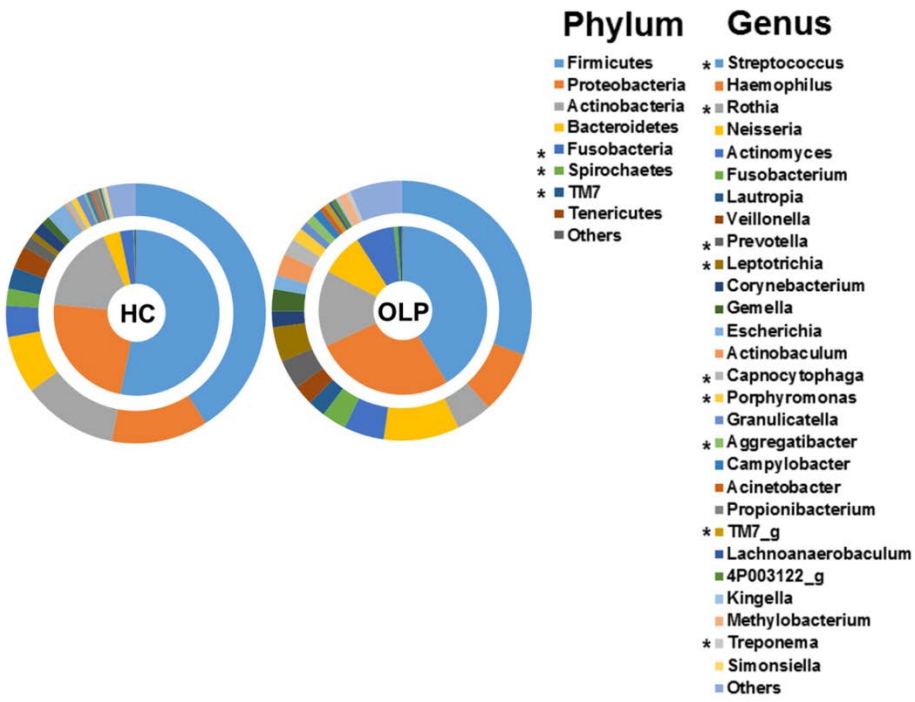

Figure 21. Comparison of the relative abundance of each taxon between healthy subjects and OLP patients. The bacterial DNA samples obtained from mucosal tissues from healthy subjects (n = 18) and OLP patients (n = 13), and the bacterial communities were analyzed pyrosequencing of amplified 16S rRNA fragments. Double pie charts present dominant phyla and genera. * indicates significant difference.

Table 5. Species/phylotypes that exhibit the significant changes of relative abundances (%)[a] in OLP compared with healthy subjects.

Species/phylotypes	Control (%) (n=18)	OLP (%) (n=13)	*P* value[b]
Fusobacterium nucleatum	0.157 (4.018, 0)	1.201 (6.187, 0.158)	0.006
Neisseria oralis	0 (0.156, 0)	0.107 (33.771, 0)	0.001
Porphyromonas gingivalis	0 (1.864, 0)	0.228 (5.048, 0)	0.018
Streptococcus gordonii	0.023 (2.538, 0)	0.595 (1.743, 0)	0.042
Leptotrichia wadei	0.015 (2.397, 0)	0.088 (3.357, 0)	0.031
Capnocytophaga gingivalis	0.030 (0.606, 0)	0.176 (2.511, 0)	0.004
Leptotrichia hongkongensis	0.034 (0.748, 0)	0.139 (1.623, 0)	0.042
Stomatobaculum longum	0.036 (0.450, 0)	0.175 (1.257, 0)	0.025
Prevotella nigrescens	0.003 (0.315, 0)	0.044 (4.664, 0)	0.031
Actinomyces naeslundii	0.012 (0.547, 0)	0.068 (2.873, 0.010)	0.028
Aggregatibacter segnis	0 (0.227, 0)	0.070 (2.570, 0)	0.005
Actinomyces meyeri	0.032 (0.200, 0)	0.161 (2.855, 0)	0.031
Eikenella corrodens	0.007 (0.216, 0)	0.056 (3.703, 0.007)	0.003
4P004975_s	0.046 (1.182, 0)	0.000 (1.119, 0)	0.014
HQ757980_s	0.072 (1.115, 0)	0.010 (0.110, 0)	0.028
Capnocytophaga sputigena	0.015 (0.528, 0)	0.148 (0.874, 0)	0.001
Parvimonas micra	0 (0.351, 0)	0.080 (0.654, 0)	0.007
Leptotrichia buccalis	0 (0.113, 0)	0.071 (3.624, 0)	0.025
Prevotella oris	0.024 (0.238, 0)	0.079 (0.461, 0)	0.014
AM420230_s	0 (1.011, 0)	0.057 (0.688, 0)	0.042
Prevotella oulorum	0 (0.830, 0)	0.023 (0.780, 0)	0.005
ADCM_s	0 (0.119, 0)	0.028 (0.653, 0)	0.038
Streptococcus vestibularis	0.016 (0.334, 0)	0.000 (0.060, 0)	0.003
Megasphaera micronuciformis	0 (0.238, 0)	0.057 (0.340, 0)	0.007
AF385572_s	0 (0.113, 0)	0.040 (0.744, 0)	0.014
Dialister invisus	0 (0.203, 0)	0.026 (0.209, 0)	0.042
Eubacterium nodatum	0 (0.264, 0)	0.024 (0.287, 0)	0.025
AF385518_s	0 (0.039, 0)	0.034 (0.382, 0)	0.012
Myxococcus virescens group	0 (0.286, 0)	0.036 (0.176, 0)	0.031
Mogibacterium vescum	0 (0.053, 0)	0.028 (0.306, 0)	0.031
Blautia wexlerae	0 (0.237, 0)	0.010 (0.321, 0)	0.031
Mogibacterium diversum	0 (0.046, 0)	0.022 (0.367, 0)	0.031
AF385506_s	0 (0.059, 0)	0.030 (0.198, 0)	0.005
Treponema denticola	0 (0.102, 0)	0.024 (0.144, 0)	0.002
Treponema socranskii	0 (0.053, 0)	0.027 (0.157, 0)	0.020
AF385554_s	0 (0.040, 0)	0.014 (0.146, 0)	0.004
AY134896_s	0 (0, 0)	0.000 (0.327, 0)	0.031
Streptococcaceae_uc_s	0.021 (0.059, 0)	0.000 (0.044, 0)	0.001
AM420042_s	0 (0.090, 0)	0.013 (0.214, 0)	0.003
Centipeda periodontii	0 (0.029, 0)	0.007 (0.443, 0)	0.025
Prevotella maculosa	0 (0.028, 0)	0.011 (0.153, 0)	0.025
Selenomonas sputigena	0 (0.037, 0)	0.022 (0.199, 0)	0.004

[a]expressed as median and range

[b]by Mann-Whitney U test

3.6. Difference of bacterial invasion, infiltrated immune cells, and microbial community between OLR and OLP

To investigate differences between OLL and OLP, the histologic features of OLL, such as an inflammatory infiltrate located deep to superficial infiltrate in some or all areas, a focal perivascular infiltrate, and the presence of either plasma cells or neutrophils in the lamina propria, are associated with any histologic parameters measured in the current study. The tissue sections with deep inflammatory infiltrate or plasma cell infiltration had increased levels of $CD8^+$ T cells in the lamina propria compared to the sections without those features. When either plasma cells or neutrophils were detected, increased levels of bacteria were observed in the lamina propria (Fig. 22a). Therefore, the cases diagnosed as OLL by one or two pathologists (OLL/OLP) had slightly higher levels of bacteria and significantly higher levels of $CD8^+$ T cells in the lamina propria than the typical OLP (OLP/OLP) cases (Fig. 22b).

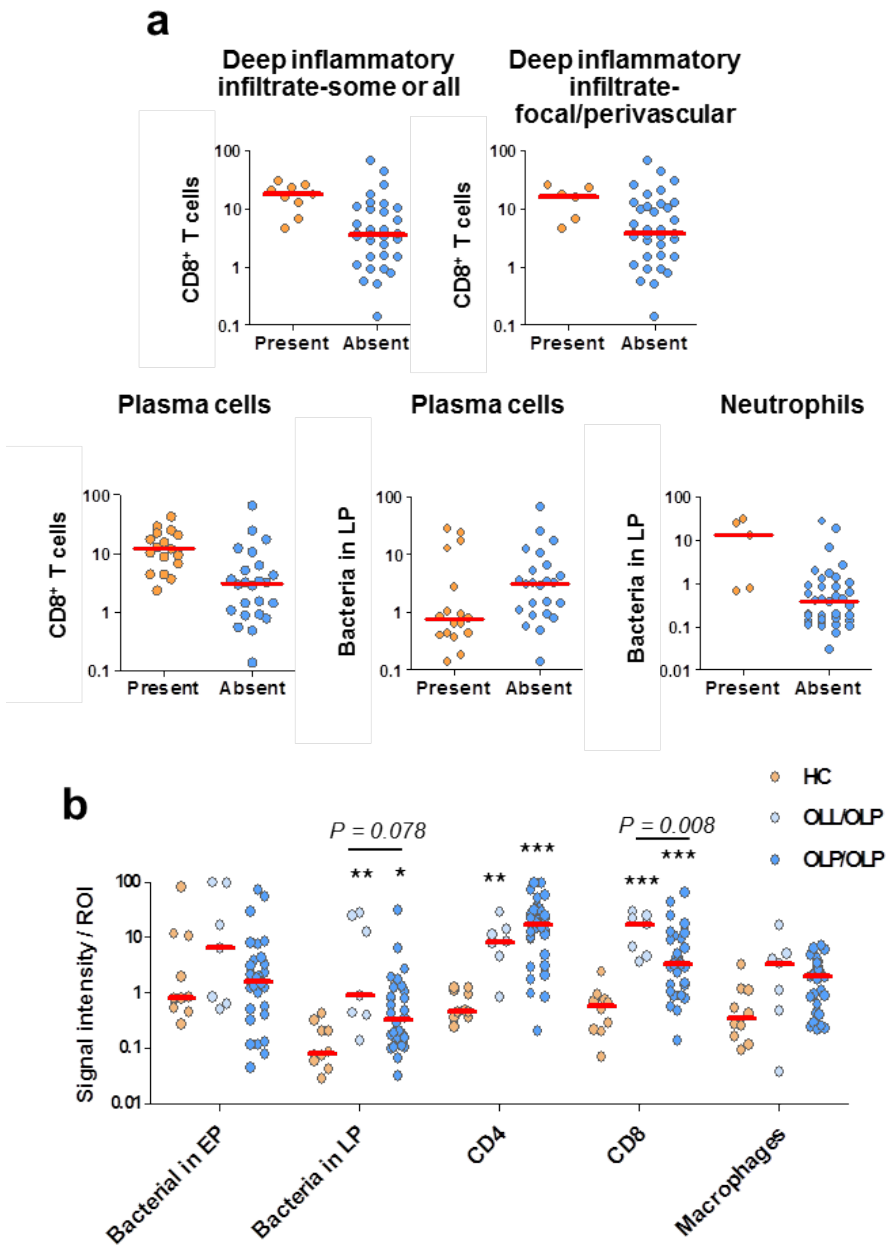

Figure 22. Differences of bacterial invasion and infiltrated immune cells

between OLL/OLP and OLP/OLP. a) Histologic features of OLL, such as an inflammatory infiltrate located deep to superficial infiltrate in some or all areas, a focal perivascular infiltrate, and the presence of either plasma cells or neutrophils in the lamina propria, are associated with any histologic parameters measured. The mean intensity of stained signals per ROI was analyzed using ImageJ software and is expressed as the median of each group. Only significant parameters ($P < 0.05$ by Mann-Whitney U test) are presented. **b)** The levels of bacterial invasion in the epithelium (EP), bacterial invasion in the lamina propria (LP), and infiltration of immune cells in the lamina propria among control (n = 10), OLL/OLP (n = 7), and OLP/OLP (n = 29) tissues were compared. *, $P < 0.05$; **, $P < 0.01$; ***, $P < 0.001$ compared with control based on the Kruskal Wallis test followed by Mann-Whitney U test with Bonferroni adjustment.

How different the OLL/OLP cases are from the OLP/OLP cases in the mucosal microbiota was also asked. In the PCoA plot, distribution of the OLL/OLP and OLP/OLP cases was not different from each other (Fig. 23). These results indicate that OLL/OLP cases have minor differences from the OLP/OLP cases in the levels of bacterial invasion into the lamina propria, infiltration of $CD8^+$ T cells, and microbial community.

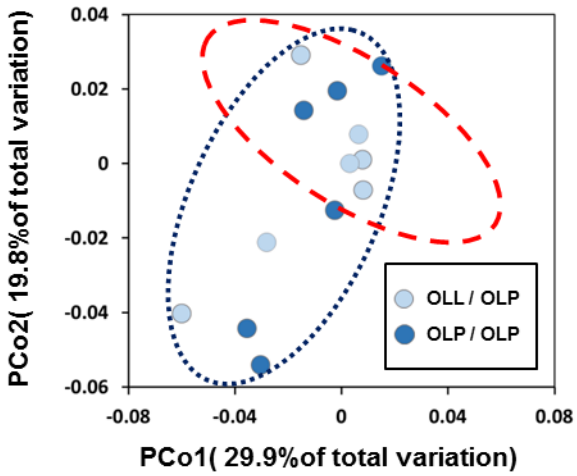

Figure 23. PCoA plot generated using weighted Unifrac metric denoting OLP/OLP and OLL/OLP cases. Red dotted line represents distribution of control samples. (Blue sky circle symbols and blue: OLL/OLP and OLP/OLP cases, respecively).

3.7. Interaction of selected bacterial species with human oral epithelial cells and leukocytes

To investigate the potential roles of bacteria in the etiopathogenesis of OLP further, the two bacterial species associated with OLP risk and *S. gordonii*, which was increased in OLP without affecting OLP risk, were chosen. Bacterial internalization into epithelial cells has an important role in the pathogenesis of diverse inflammatory diseases. An internalization of *S. sanguinis* and *S. gordonii* into human oral keratinocyte (HOK)-16B cells was previously reported (Ji et al., 2007). However, internalization of *C. gingivalis* has not been studied in HOK-16B cells. Therefore, the internalization of *C. gingivalis* into HOK-16B cells was investigated by confocal microscopy. CFSE-labeled *C. gingivalis* was detected within the cell boundary surrounded by actin filaments of HOK-16B cells (Fig. 24a). To quantify amounts of *C. gingivalis* internalization into HOK-16B cells, the infected cells were also analyzed by flow cytometry. *C. gingivalis* has a substantial capacity of internalization into HOK-16B cells (Fig. 24b). Diverse pathogens are known to modulate physical barrier function of epithelia to facilitate their infection (Cereijido et al., 2007; Chi et al., 2003; Katz et al., 2002; Salim and Soderholm, 2011). Therefore, the effect of bacteria on the physical barrier function was further determined by measuring transepithelial electrical resistance (TER) of immortalized HOK-16B cells cultured on a porous

membrane. Only *C. gingivalis* induced a significant decrease in TER in a time dependent manner without affecting the viability of HOK-16B cells (Fig. 24c-d). These results indicate that *C. gingivalis* can get inside into HOK-16B cells, and modulate the epithelial barrier functions.

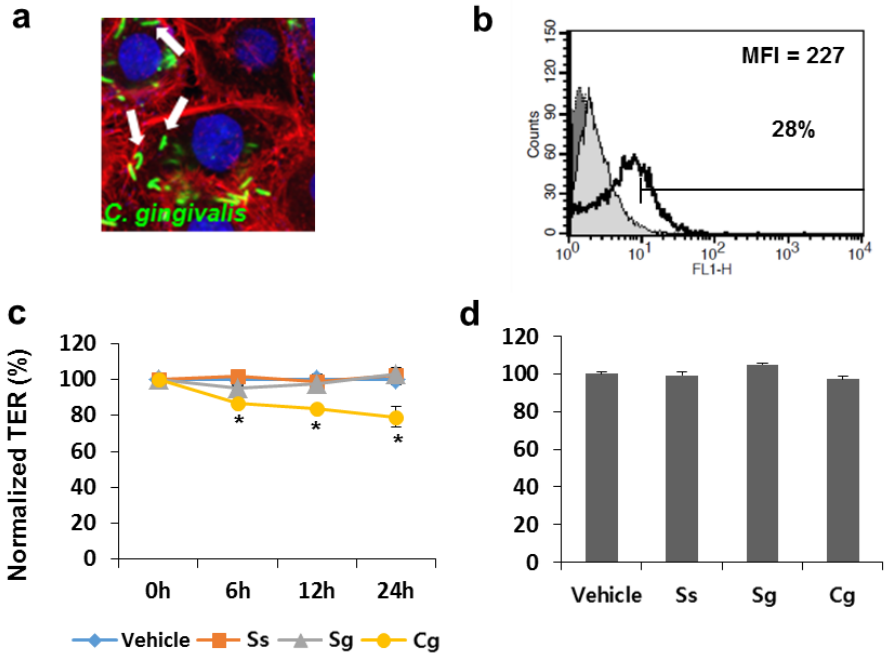

Figure 24. Internalization into HOK-16B cells and modulation of epithelial physical barrier by *C. gingivalis*. a) HOK-16B cells were plated and were infected with CFSE-labeled *C. gingivalis* (green) at an MOI of 1000 for 24 h. After fixation, cells were stained with Hochest 33342 and rhodamine-phalloidin, and then examined by confocal microscopy. White

arrows indicate bacteria within the cell boundary. Blue, Hoechst 33342; red, rhodamine phalloidin. Scale bar, 10 μm. **b)** HOK-16B cells containing internalized CFSE-labeled *C. gingivalis* (thick empty line) analyzed by flow cytometry were overlaid over negative controls (dark gray, fixed cells infected with bacteria; light gray, non-infected live cells) **c)** Tight-junctioned monolayers of HOK-16B cells were infected with *S. sanguinis* (Ss), *S. gordonii* (Sg), and *C. gingivalis* (Cg) at an MOI of 500. TER was measured at 0, 6, 12, and 24 h. The means ± the SEM of measured TER are expressed as the relative percentage compare to baseline (n = 6 wells in 2 experiments). *, $P < 0.05$ (Two-tailed non-paired Student's t-test) **d)** Tight-junctioned monolayers of HOK-16B cells were infected with *S. sanguinis* (Ss), *S. gordonii* (Sg), and *C. gingivalis* (Cg). After 24 h infection, cell viability was measured using a CCK-8 assay kit. The means ± the SEM measured cell viability are expressed (n = 6 wells in 2 experiments). *, $P < 0.05$ (Two-tailed non-paired Student's t-test)

Next, this study explored whether the selected bacterial species can be internalized into T cells, as observed in the biopsied tissues. The purified human $CD4^+$, $CD8^+$, or $CD14^+$ cells were infected with 5- and 6-carboxy-fluorescein diacetate succinimidyl ester (CFSE, green)-labeled bacteria for one hour and examined by confocal microscopy. Surprisingly, all three species were detected within the cell boundary surrounded by actin filaments of both $CD4^+$ and $CD8^+$ cells as well as within the $CD14^+$ cells (Fig. 25a). To exclude the possibility that the bacteria-containing cells in the either $CD4^+$ or $CD8^+$ populations are a few contaminating monocytes, the infected cells were also analyzed by flow cytometry with gating on the lymphocytes after quenching the fluorescence of bacteria bound on the cell surface. *S. sanguinis* and *S. gordonii* were internalized into both $CD4^+$ and $CD8^+$ cells in substantial levels, while the levels of *C. ginigivalis* internalization into either $CD4^+$ or $CD8^+$ cells were low (Fig. 25b).

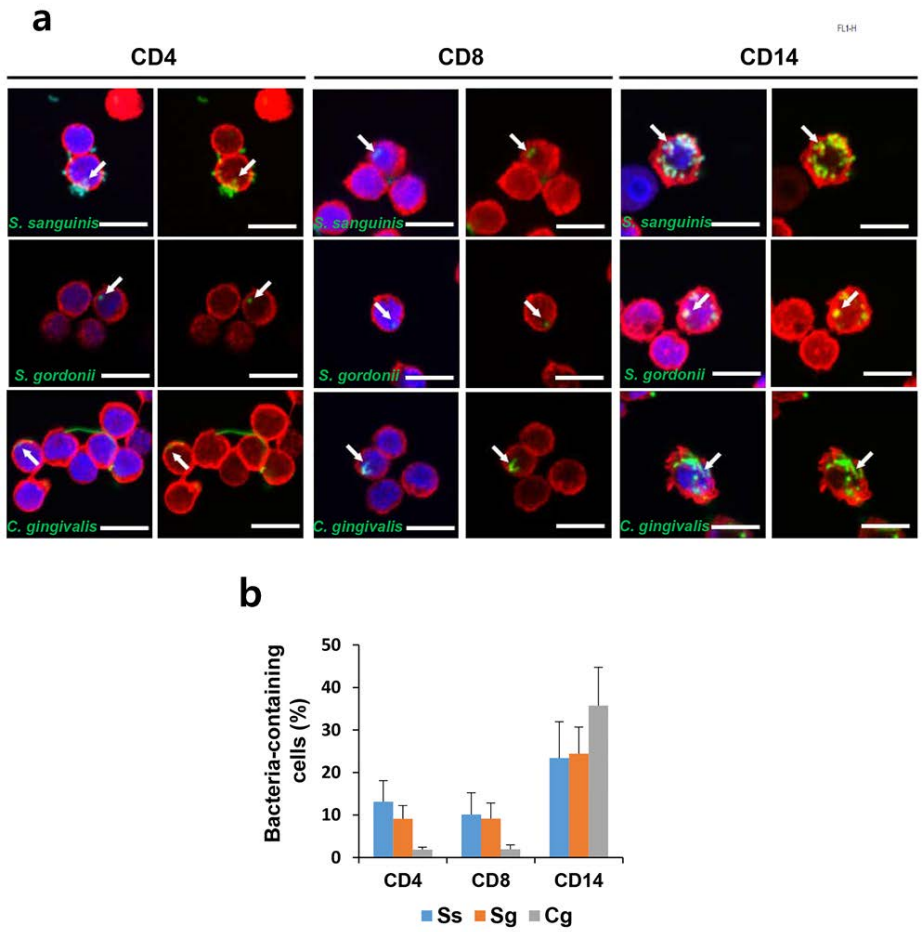

Figure 25. Bacterial internalization into CD4 $^{+}$, CD8 $^{+}$, and CD14^{+} cells. Purified human CD4^{+}, CD8^{+}, or CD14^{+} cells were plated (n = 3 different donors). The cells were infected with CFSE-labeled bacteria at an MOI of 1000 in RPMI without antibiotics for 1 h. **a)** After fixation, cells were stained with Hochest 33342 and rhodamine-phalloidin, and then examined by confocal microscopy with serial Z-sections. The bacteria signals marked with white arrows. Blue, Hoechst 33342; red, rhodamine phalloidin; green, CFSE.

Scale bar, 10 μm. **b)** The cells were infected with CFSE-labeled *S. sanguinis* (Ss), *S. gordonii* (Sg), and *C. gingivalis* (Cg) at an MOI of 1000 in RPMI without antibiotics for 1 h. After washing with PBS, the fluorescence of the bacteria bound on the surface were quenched by trypan blue. The bacterial internalization was examined by flow cytometry. The means ± the SEM are expressed.

Whether the internalized bacteria survive within the cells or not was examined by an antibiotics protection assay. The cells were infected with selected bacteria without antibiotics for 1 h, and the infected cells were treated with gentamycin and then further cultured for 1 or 24 h. After 1 or 24 h treatment with gentamycin, the lysate of infected cells was directed cultured on blood agar. Although all selected bacteria could survive within $CD4^+$, $CD8^+$ and $CD14^+$ cells after 1 h treatment of gentamycin, the number of *C. ginigivalis* within $CD14^+$ cells was significantly higher than other bacteria (Fig. 26). After 24 h treatment of gentamycin, only *C. ginigivalis* within $CD14^+$ cells still survived (Fig. 26). These results suggest that bacteria can get inside into immune cells, including T cells, and *C. ginigivalis* can still survive within $CD14^+$ cells for 24 h.

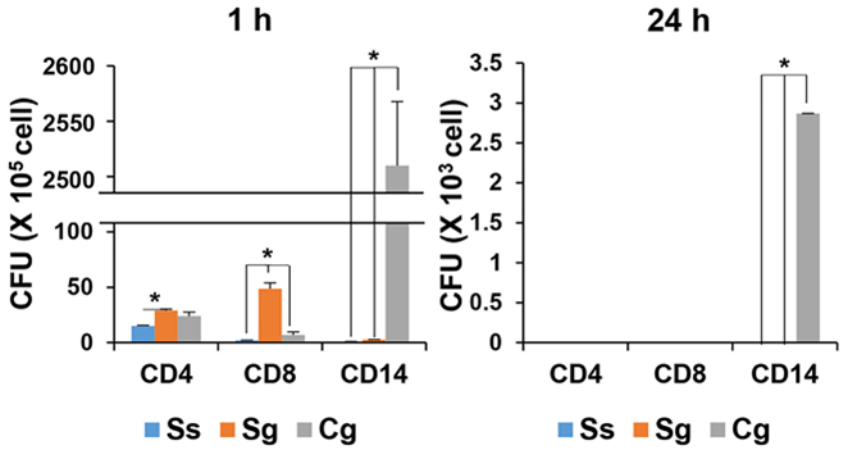

Figure 26. Bacterial survival within CD4$^+$, CD8$^+$, and CD14$^+$ cells. Purified human CD4+, CD8+, or CD14+ cells were infected with bacteria at MOI 1000 for 1 hour and further cultured for 1 and 24 hours in the presence of gentamicin. After lysing the cells, bacteria in the lysates were cultured on blood agar plates. The number of bacteria that survived within the cells are expressed as a colony forming unit (CFU). The means ± the SEM are expressed. *, $P < 0.05$ (One-way ANOVA with Tukey's post hoc).

Increased levels of chemokines, including CCL3 (MIP-1α), CCL5 (RANTES), CXCL8 (IL-8), and CXCL10 (IP-10) have been implicated in the recruitment of immune cells. To investigate the role of bacteria in the pathogenesis of OLP, the levels of these chemokines in the medium of HOK-16B, $CD4^+$, $CD8^+$, and $CD14^+$ cells infected with the three bacterial species were measured by ELISA. Upon bacterial challenge, $CD14^+$ cells most efficiently induced all four chemokines. $CD4^+$ cells also produced CCL3 and CXCL8 at high levels and CCL5 and CXCL10 at substantial levels. $CD8^+$ cells upregulated only CCL3 and CCL5 at low levels and HOK-16B cells barely responded to bacterial challenge (Fig. 27). These results suggest that chemokine can be produced by immune cells in response to bacteria.

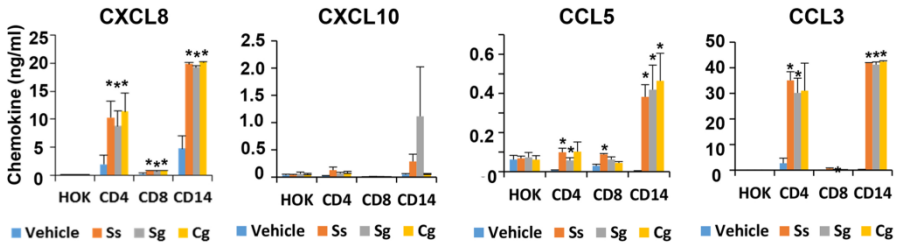

Figure 27. The levels of chemokines in the medium of infected cells with selected bacteria. The amounts of CXCL8, CXCL10, CCL5, and CCL3 in culture supernatant of HOK-16B cells, $CD4^+$, $CD8^+$, or $CD14^+$ cells infected with bacteria at MOI 1000 for 1 hour and further cultured for 24 hours with gentamicin. **a)** The amounts of CXCL8 secreted into the medium during infection with selected bacteria were measured using ELISA. **b)** The amounts of CXCL10, CCL5, and CCL3 were determined using Multiplex assay. The means ± the SEM are expressed (n = 3 different donors). *, $P < 0.05$ (Two-tailed non-paired Student's t-test).

3.8. Enhanced physical barrier function by 17β-estradiol under the normal condition

To investigate the effect of 17β-estradiol on the epithelial physical barrier, HOK-16B cells were plated onto a 3μm-pore-size polycarbonate filter of a 24-well plate of the transwell two-chamber tissue culture system one day

before 17β-estradiol treatment, and then cells were treated with 0.2-20 nM 17β-estradiol for 0, 6, 12, 24, 48, 72, or 96 h. The treatment of 17β-estradiol had no significant effect on the proliferation of HOK-18B cells compared with vehicle control (Fig. 28a). However, cells treated with 17β-estradiol showed increased the TER values in a time-dependent and dose-dependent manner until 72 h (Fig. 28b). 20 nM 17β-estradiol significantly enhanced the TER values at 6 and 24 h (Fig. 28b). After reaching maximal value 72 h, TER was decreased (Fig. 28b). These data suggest that 17β-estradiol enhanced the epithelial physical barrier under the normal condition.

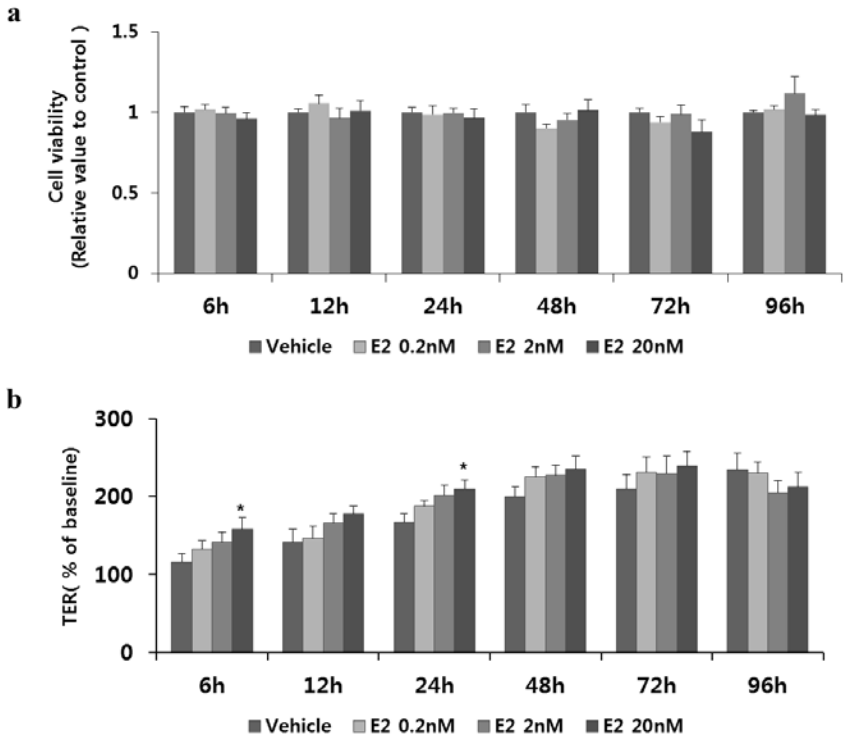

Figure 28. Enhanced physical barrier function by 17β-estradiol under the normal condition. a) HOK-16B cells were plated, and then were treated with 17β-estradiol (E2). The proliferation of HOK-16B cells was measured using CCK-8 assay kit at indicated time points (n = 6 wells in 2 experiments). The means ± the SEM of measured absorbance are expressed as the relative index compare to baseline. **b)** HOK-16B cells were plated onto a 3μm-pore-size polycarbonate filter of a 24-well plate of the transwell two-chamber tissue culture system one day before 17β-estradiol treatment, and then cells were treated with 17β-estradiol (0.2-2 nM). TER was measured at indicated time

points (n = 6 wells in 2 experiments). The means ± the SEM of measured TER are expressed as the relative percentage compare to baseline. *, $P < 0.05$ (Two-tailed non-paired Student's t-test)

The expression levels of TJ proteins, including ZO-1 and JAM-A, have been implicated in physical barrier function. To investigate the effect of 17β-estradiol on the formation of TJ proteins, whether 17β-estradiol could induce the expression of TJ proteins was analyzed using a confocal microscopy. 20 nM 17β-estradiol significantly induced increased levels of ZO-1 and JAM-A compared with vehicle control at 24 h (Fig. 29a-b). However, the gene levels of TJ proteins were not different (Fig. 29.c-d). These data indicate that 17β-estradiol enhanced the epithelial physical barrier through up-regulation of TJ proteins.

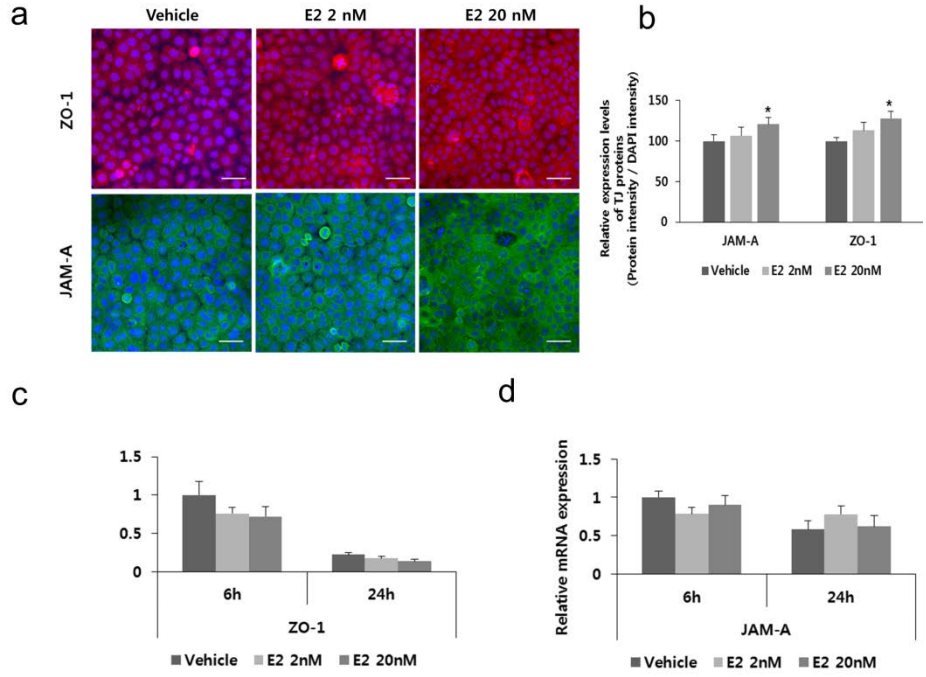

Figure 29. Increased proteins levels of TJ-proteins by 17β-estradiol under the normal condition. HOK-16B cells were plated and then were treated with 2 nM or 20 nM 17β-estradiol for 24 h. **a-b)** After fixation, cells were stained with ZO-1 and JAM-A. The fluorescence intensity of ZO-1 and JAM-A was analyzed and normalized to the fluorescence intensity of Hochest 33342. The means ± the SEM of fluorescence intensity are expressed as the relative percentage compared with vehicle control. **c-d)** After 24 h treatment of 17β-estradiol, the gene levels of TJ-proteins were evaluated by real-time RT-PCR. The means ± the SEM of real-time RT-PCR assay are expressed as the relative index compare to vehicle control (n = 6 wells in 2 experiments). *, $P < 0.05$ (Two-tailed non-paired Student's t-test)

3.9. Disruption of physical barrier function by TNF-α

Previous study reported that pro-inflammatory cytokine TNF-α could induce the disruption of physical barrier (Kimura et al., 2008). To determine the effect of TNF-α on gingival epithelial barrier functions, tight-junctioned monolayers of HOK-16B cells were treated with treatment of 10-250 ng/ml TNF-α. The TER values of TNF-α treatment were decreased in a time-dependent manner (Fig. 30a) at 24 h, TER values were significantly decreased compared with vehicle control (Fig. 30a). However, cells were treated with 250 ng/ml TNF-α showed increased cell death (Fig. 30b). To avoid increased cell death by TNF-α treatment, HOK-16B cells were treated with 10 or 100 ng/ml TNF-α in the observation of TJ proteins expression. TNF-α reduced the levels of ZO-1 and JAM-A at 24 h (Fig. 30c). These results suggest that TNF-α induces the disruption of gingival epithelial barrier functions through decreased levels of TJ proteins.

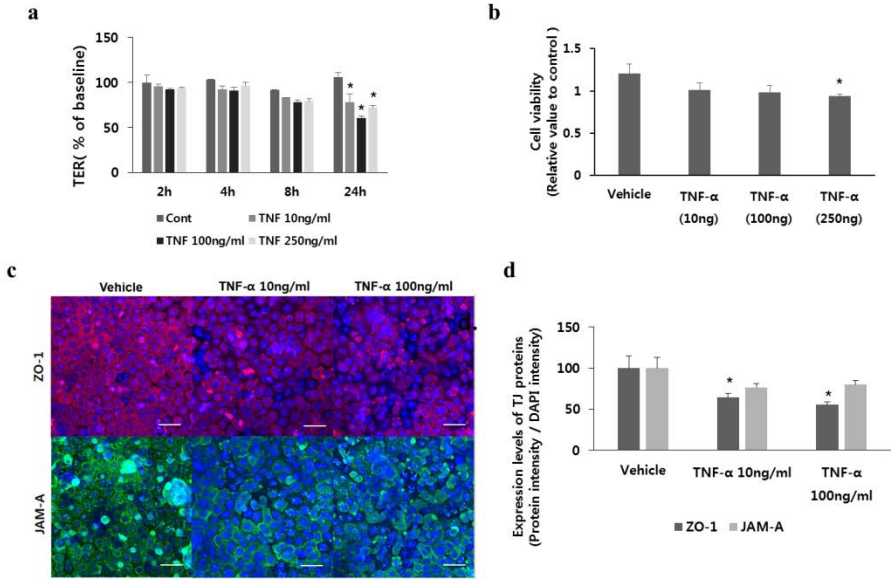

Figure 30. Disruption of physical barrier by TNF-α. Tight-junctioned monolayers of HOK-16B cells were treated with TNF-α (10 - 250 ng/ml) for 24 h. **a)** TER was measured at indicated time points. The means ± the SEM of TER are expressed as the relative percentage compare to baseline (n = 3). **b)** Cell viability was measured using CCK-8 assay kit at indicated time points. The means ± the SEM of measured absorbance are expressed as the relative index compare to baseline (n = 6 wells in 2 experiments). **c-d)** After fixation, cells were stained with for ZO-1 and JAM-A. The fluorescence intensity of ZO-1 and JAM-A was analyzed and normalized to the fluorescence intensity of Hochest 33342. The means ± the SEM of fluorescence intensity are expressed as the relative percentage compare to vehicle control (n = 10 data points). *, $P < 0.05$ (Two-tailed non-paired Student's t-test)

3.10. Protective effect of 17β-estradiol on TNF-α induced-damaged epithelial physical barrier.

To investigate effect of 17β-estradiol on the gingival epithelial barrier under the pro-inflammatory cytokine-induced damaged condition, tight-junctioned monolayers of HOK-16B cells were pre-treated with either 17β-estradiol (2-20 nM) or ICI 182,780 (125 μM) before treatment of TNF-α (100 ng/ml). TER was measured at 24 h. TNF-α reduced the TER values, but 17β-estradiol protected TNF-α-induced epithelial damage (Fig. 31a). However, ICI 182,780 blocked the protective effects of 17β-estradiol (Fig. 31a). In all experimental groups, cell viability was not different (Fig. 31b). These results indicate that 17β-estradiol can protect TNF-α-induced epithelial damage.

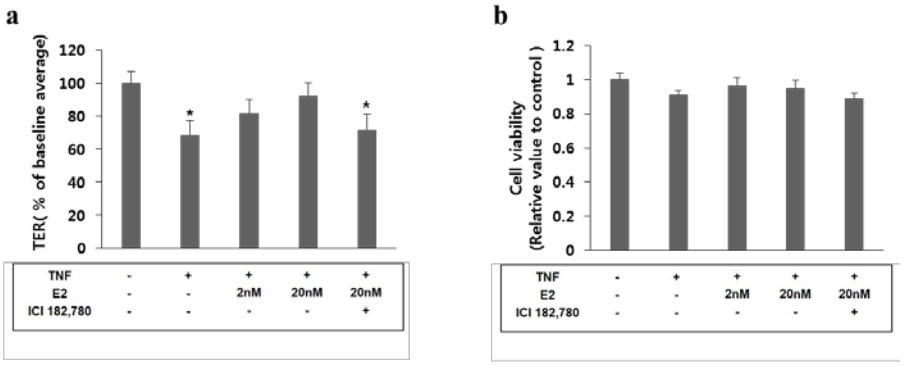

Figure 31. Protective effect of 17β-estradiol on TNF-α induced-damaged epithelial physical barrier. Tight-junctioned monolayers of HOK-16B cells were pre-treated with either ICI 182,780 (125 μM) for 2 h or 17β-estradiol (2-20 nM) for 4 h before treatment with TNF-α (100 ng/ml) for 24 h. **a)** TER was measured at 24 h (n = 3). The means ± the SEM of measured TER are expressed as the relative percentage compare to baseline. **b)** Cell viability was measured using CCK-8 assay kit at indicated time points (n = 6 wells in 2 experiments). The means ± the SEM of measured absorbance are expressed as the relative index compare to baseline. *, $P < 0.05$ (Two-tailed non-paired Student's t-test)

To investigate protective effect of 17β-estradiol on the alteration of TJ proteins under the pro-inflammatory cytokine-induced damaged condition, the expression of TJ proteins was analyzed using a confocal microscopy. Similar to physical barrier functions, TNF-α reduced the expression levels of ZO-1, but 17β-estradiol protected reduction of ZO-1 protein levels (Fig. 32a-b). However, ICI 182,780 blocked the protective effects of 17β-estradiol (Fig. 32a-b). The gene levels of TJ proteins were not associated with the levels of TER and TJ proteins (Fig. 32c-d). These results support that 17β-estradiol has a protective effect of 17β-estradiol on decreased levels of TJ-proteins by TNF-α.

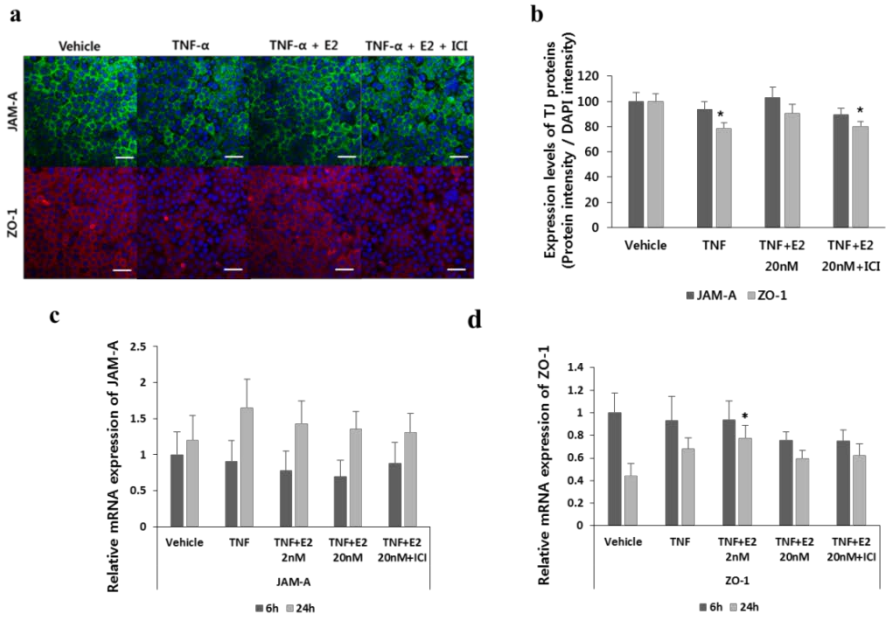

Figure 32. Protective effect of 17β-estradiol on decreased levels of TJ-proteins by TNF-α. Tight-junctioned monolayers of HOK-16B cells were pre-treated with either ICI 182,780 (125 μM) for 2 h or 17β-estradiol (2-20 nM) for 4 h before treatment with TNF-α (100 ng/ml) for 6 or 24 h. **a-b)** After fixation, cells were stained with ZO-1 and JAM-A. The fluorescence intensity of ZO-1 and JAM-A was analyzed and normalized to the fluorescence intensity of Hochest 33342. The means ± the SEM of fluorescence intensity are expressed as the relative percentage compare to vehicle control (n = 20 data points in 2 experiments). **c-d)** After 6 or 24 h treatment of TNF-α, the gene levels of TJ-proteins ZO-1 and JAM-A were evaluated by real-time RT-PCR (n = 9 wells in 3 experiments). The means ± the SEM of real-time

RT-PCR assay are expressed as the as the relative index compare to vehicle control. *, $P < 0.05$ (Two-tailed non-paired Student's t-test)

3.11. Inhibition of NF-κB nuclear translocation by 17β-estradiol in the TNF-α induced-damaged epithelial physical barrier.

The anti-inflammatory response of estrogens through inhibition of NF-κB nuclear translocation has been reported (Kalaitzidis and Gilmore, 2005). To investigate anti-inflammatory response of 17β-estradiol in the gingival epithelial cells, NF-κB nuclear translocation was observed using a confocal microscopy under the TNF-α-induced damaged condition. In the vehicle control, almost positive signals of NF- κB were located within cytoplasm (Fig. 33a-b). However, TNF-α treatment induced the NF-κB nuclear translocation (Fig. 33a-b). Interestingly, NF-κB nuclear translocation by TNF-α was inhibited by pre-treatment of 17β-estradiol (Fig. 33a-b). However, ICI 182,780 blocked the protective effects of 17β-estradiol (Fig. 33a-b). These results showed that 17β-estradiol inhibited NF-κB nuclear translocation.

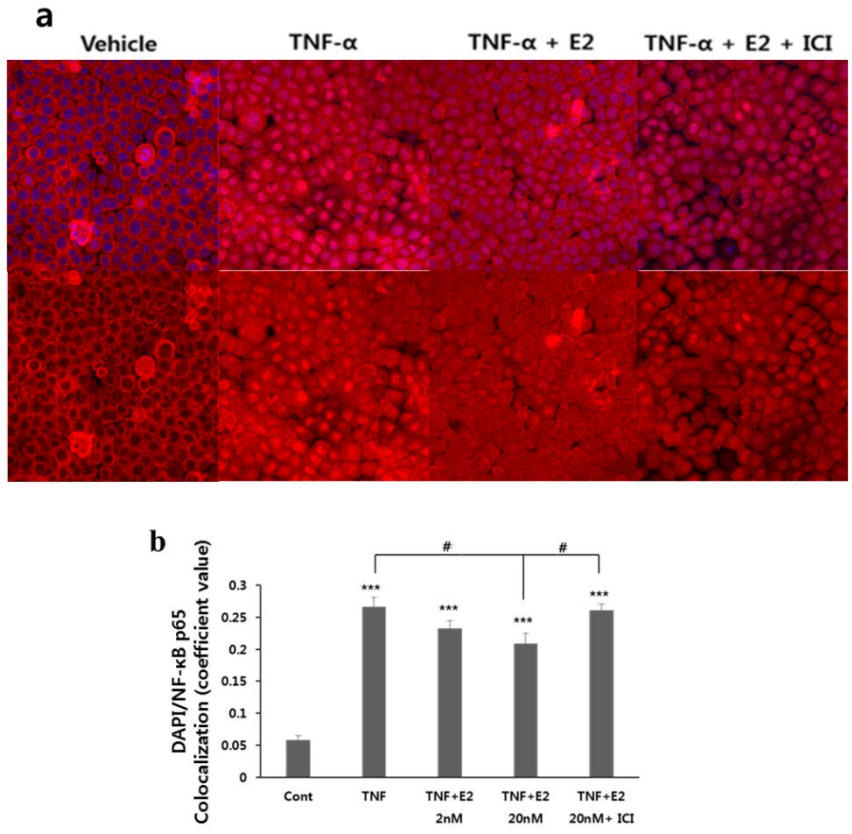

Figure 33. Inhibition of NF-κB nuclear translocation by 17β-estradiol in the TNF-α induced-damaged epithelial physical barrier. a-b) Tight-junctioned monolayers of HOK-16B cells were pre-treated with either ICI 182,780 (125 μM) for 2 h or 17β-estradiol (2-20 nM) for 4 h before treatment with TNF-α (100 ng/ml) for 30 minutes. After fixation, cells were stained with NF-κB p65. For quantification of nuclear translocation of NF-κB, co-localized signals of nucleus and NF-κB p65 were measured. The means ±

the SEM are expressed (n = 30 data points in 3 experiments). *, $P < 0.05$; # $P < 0.05$ (One-way ANOVA with Tukey's post hoc).

Chapter IV. Discussion

The present study demonstrated that bacterial invasion into the mucosal tissues was increased in OLP tissues, which was strongly associated with the infiltration of $CD4^+$ and $CD8^+$ T cells. Furthermore, this study provided evidence that certain bacteria can invade both $CD4^+$ and $CD8^+$ T cells within the mucosal tissues. Pyrosequencing analysis revealed an alteration of oral microbiota in OLP, and discovered that *C. gingivalis* was associated with increased OLP risk. In addition, all selected bacteria had the ability to internalize into $CD4^+$, $CD8^+$, and $CD14^+$ cells *in vitro*, and *C. gingivalis* could survive within $CD14^+$ cells for 24 h. Moreover, *C. gingivalis* could modulate the epithelial barrier function, and all selected bacteria could induce chemokines. Indeed, the present study demonstrated that the interaction between oral bacteria and the host immune system had a potential role in OLP.

The disruption of physical barriers allows for the invasion of commensal bacteria into tissue and chronic inflammation. A preliminary study of animal models showed a strong correlation between bacterial invasion and

the infiltration of $CD3^+$ T cells (Choi et al., 2013). In the present study, bacterial invasion also had a strong positive correlation with infiltrated $CD4^+$ and $CD8^+$ cells within the lamina propria. Therefore, the strong correlation between bacterial invasion and T cell infiltration suggests an important role for bacterial invasion in OLP. In addition, diverse pathogens including periodontal pathogens can regulate the epithelial physical barrier to invade host cells and/or tissues by damage or remodeling TJ-proteins (Chi et al., 2003; Choi et al., 2013; Dickman et al., 2000; Katz et al., 2002; Nusrat et al., 2001). Although the levels or distribution of TJ-proteins have not been studied, the OLP epithelium is characterized by its abnormal structure including the degeneration/destruction of epithelial cells. This study found that *C. gingivalis* can induce decreased levels of TER, and it may degrade proteins or large peptides because it has a trypsin-like protease (Spratt et al., 1995) similar to the gingipain of *P. gingivalis.*

Although $CD8^+$ T cells are regarded as mediating the degeneration/destruction of epithelial cells, it is unknown what triggers the infiltration of T cells in OLP. Pyrosequencing data revealed that periodontal pathogens including *P. gingivalis* and *T. denticola* were increased in OLP. Diverse periodontal pathogens can invade epithelial cells (Lamont and Yilmaz, 2002; Meyer et al., 1996; Njoroge et al., 1997; Yilmaz et al., 2002). Both *P. gingivalis* and *A. actinomycetemcomitans* can invade epithelial cells, and can

then spread into neighboring cells (Griffen et al., 2012; Ji et al., 2014; Madianos et al., 1996). Indeed, the present study determined that bacteria were internalized within the basal layer of the epithelia in OLP tissues. In addition, bacterial invasion into the basal layer of the epithelia was more frequently detected in OLP tissues compared to the control, and OLP-related bacteria *C. gingivalis* could also invade epithelial cells. Therefore, infected epithelial cells would be a target of infiltrated cytotoxic $CD8^+$ T cells.

Multiple studies have reported that the dysbiosis of microbial composition induced inflammation and tissue destruction, leading to oral infectious diseases such as dental caries, periodontitis, and gingivitis (Griffen et al., 2012; Murakami et al., 2004; Park et al., 2015; Pflughoeft and Versalovic, 2012). In the present study, increased microbial diversity and changes to the microbial composition in OLP were shown. This evidence suggests that a changed microbial community is associated with OLP. A similar change has been shown in the microbiota of subgingival biofilm in patients with periodontitis (Park et al., 2015). In addition, a previous study by the present author demonstrated that the microbial composition of the oral cavity was shifted by alterations to the epithelial environment such as increased pathogens and damaged physical barrier (Choi et al., 2013). Multiple studies were also presented that changed the host environment [e.g., pH or nutrients] could increase the relative abundances of pathogens

(Dethlefsen et al., 2007; Hanin et al., 2010; Kolenbrander et al., 2010). This study did not answer the question of whether the dysbiosis of oral microbiota is a cause or a result of OLP; nevertheless, the present study can speculate that both the dysbiosis of microbiota and environmental alteration of the epithelia, such as an increase of invasive bacteria or damaged epithelia, may contribute to increased bacterial invasion into the mucosal tissues.

Chronic inflammation is associated with persistent infection, including the failed clearance of invaded pathogens due to an inadequate immune response and continuous bacterial invasion into host tissues (Ji et al., 2014). Here, the present study showed that certain oral bacteria were detected in both $CD4^+$ and $CD8^+$ T cells within OLP tissues. It is surprising that lymphocytes are not phagocytic cells. Interestingly, one group reported that *Shigella flexneri* can directly invade T cells by a type three secretion system (T3SS) that inhibits T cell dynamics (Konradt et al., 2011; Salgado-Pabón et al., 2013). In the present study, all selected bacterial species were also internalized into $CD4^+$, $CD8^+$, and $CD14^+$ cells *in vitro*. A previous study reported that infiltrated $CD8^+$ T cells within OLP tissues expressed CCL5, CXCL10, and their receptors in the cytoplasm, suggesting a mechanism of self-recruitment (Iijima et al., 2003). In the present study, T lymphocytes including $CD4^+$, $CD8^+$, and $CD14^+$ cells could produce CCL5 by bacterial challenge. Furthermore, $CD4^+$ and $CD14^+$ cells produced macrophage

chemokine CCL3 via bacterial challenge. It can be expected that infiltrated T cells in OLP lesions may produce CCL5 and CCL3 by infiltrating bacteria into tissues. Because CXCL8 is well known as a chemoattractant for neutrophils (Himmel et al., 2011), the induction of CXCL8 from T cells was not expected. However, the stimulation of purified $CD14^+$ cells and T cells with bacteria also induced CXCL8. Generally, neutrophils are recruited to kill extracellular bacteria during an acute infection (Kolaczkowska and Kubes, 2013). Therefore, one possible reason for the absence of neutrophils in OLP tissues is that bacterial signals might be detected within cells. In addition, OLP is a chronic inflammatory disease, which may explain why OLP lesions do not include the infiltration of neutrophils. Collectively, these results indicate that increased levels of chemokine from infiltrated immune cells by bacterial challenge would be the main cause of chronic inflammation in OLP. Nonetheless, the present study did not prove the molecular mechanisms associated with bacterial invasion into T lymphocytes and the precise role of bacteria within mucosal tissues. Therefore, the precise role and molecular mechanisms of bacteria require further investigation.

This study divided clinically diagnosed OLP into OLP/OLP and OLL/OLP cases according to the negative features of pathological characteristics (Thornhill et al., 2006). In the present study, the levels of infiltrated $CD8^+$ T cells were increased in OLL/OLP cases compared to

OLP/OLP cases. In contrast, $CD4^+$ T cells were increased in OLP/OLP cases, although not to a significant level. Interestingly, in the case of $CD4^+/CD8^+$, value was significantly increased in OLP/OLP cases compared to OLL/OLP (15.217 ± 7.180 vs. 0.872 ± 0.295, P = 0.008). The increased $CD4^+/CD8^+$ value of the other study has also been shown in OLP (JB et al., 1984) similar to the result of the present study. Similar to OLL, chronic junctional stomatitis (CJS) is another similar condition characterized by infiltrated T cells, which is a pathological feature of OLP. A previous study reported that the ratio of $CD4^+/CD8^+$ T cells is also higher within OLP than CJS (Omar et al., 2009). In the present study, OLL/OLP cases had increased levels of bacterial signals in the epithelia and lamina propria compared to OLP/OLP cases. One possibility is that the differences in the bacterial burden and localization within tissues may make differences in the OLL/OLP and OLP/OLP cases in the immune cell infiltration levels. However, OLL/OLP cases had minor differences from OLP/OLP cases in the composition of mucosal microbiota. In addition, the PCoA plot distributions of OLL/OLP and OLP/OLP cases almost matched. Collectively, these results indicate that although OLL/OLP and OLP/OLP have some differences, the interaction between oral bacteria and the host immune system has an important role in the progress of both diseases.

Under normal conditions, 17β-estradiol enhanced the epithelial physical barrier, and induced increased levels of TJ proteins. Furthermore, the

pretreatment of 17β-estradiol protected against the disruption of the epithelial physical barrier function through maintaining the expression levels of TJ protein. In addition, 17β-estradiol inhibited NF-κB nuclear translocation via the pro-inflammatory cytokine TNF-α.

In the present study, 17β-estradiol enhanced the epithelial physical barrier and induced increased levels of TJ proteins under normal or damaged conditions. Similar to the present study, estradiol modulates colonic physical barrier functions via the up-regulation of occludin and JAM-A through ERβ signaling (Braniste et al., 2009). In addition, estradiol inhibits the disruption of the blood brain barrier via ischemia re-perfusion in female rat (Chotirmall et al., 2010). However, the gene levels of ZO-1 and JAM-A were not associated with these protein levels. Similar to the present study, Kwak et al. reported that the *S. aureus alpha-toxin* reduces the proteins levels of ZO-1 and ZO-3, but induces increased gene levels of these proteins at the same time (Kwak et al., 2012). One possibility is that TJ proteins are rapidly degraded or regulated at translation rather than transcription. Another possibility is that the increased gene levels of TJ proteins may reflect a compensatory response in an attempt to repair the damaged epithelial barrier, and the decreased gene levels of JAM-A and ZO-1 over the normal condition period support this possibility.

The anti-inflammatory responses of estrogen have been shown in multiple studies; 17β-estradiol regulates interleukin (IL)-1β-mediated pro-inflammatory responses in uterine epithelial cells (Schaefer et al., 2005). Similarly, 17β-estradiol has the inhibitory function of IL-8 in cyclic fibrosis (Chotirmall et al., 2010). In addition, 17β-estradiol inhibited NF-κB nuclear translocation in gingival epithelial cells under the pro-inflammatory cytokine-induced damaged condition in the present study. These findings suggest that estrogen may protect against the progression of chronic inflammatory diseases including OLP and periodontitis by regulating physical barrier functions and inflammatory responses.

The present study did not find the specific molecular mechanism for 17β-estradiol in TJ formation. However, previous studies have reported that the mitogen-activated protein kinases (MAPK) signaling pathway is associated with TJ formation in diverse epithelial cells (Dorfel and Huber, 2012; Gonzalez-Mariscal et al., 2008; Wang et al., 2004). Similarly, estrogen enhances the expression levels of occludin in human umbilical vein endothelial cells through the MAPK signaling pathway (Sumanasekera et al., 2007; Sumanasekera et al., 2006). Therefore, one possibility is that estrogen may have enhanced the gingival epithelial physical barrier by increasing levels of TJ proteins through the MAPK signaling pathway. Although the present study did not find the specific mechanism, the inhibition of the NF-κB

signaling pathway has been shown via diverse mechanisms through ER activation (Kalaitzidis and Gilmore, 2005; Xing et al., 2009). Estrogen enhances the expression levels of the inhibitor of kappa (IκB) and inhibits the phosphorylation and degradation of IκBα through ER activation (Kalaitzidis and Gilmore, 2005). In addition, ER activation enhances the stabilization of IκBα to inhibit I kappa B kinase (IKK) (Kalaitzidis and Gilmore, 2005), and estrogen induces direct interaction with NF-κB in the nucleus via ER (Xing et al., 2009). Therefore, 17β-estradiol may inhibit NF-κB nuclear translocation through ER activation.

In conclusion, increased bacterial invasion into mucosal cells/tissues and altered microbial communities may contribute to the etiopathogenesis of OLP. Maintaining the epithelial physical barrier could be targeted by 17β-estradiol to prevent bacterial invasion into tissues and reduce the occurrence of OLP.

Chapter V. References

1. Blasco-Baque, V., Serino, M., Vergnes, J.N., Riant, E., Loubieres, P., Arnal, J.F., Gourdy, P., Sixou, M., Burcelin, R., and Kemoun, P. (2012). **High-fat diet induces periodontitis in mice through lipopolysaccharides (LPS) receptor signaling: protective action of estrogens.** PLoS One 7, e48220.

2. Boehringer, H., Taichman, N.S., and Shenker, B.J. (1984). **Suppression of fibroblast proliferation by oral spirochetes.** Infect Immun 45, 155-159.

3. Braniste, V., Leveque, M., Buisson-Brenac, C., Bueno, L., Fioramonti, J., and Houdeau, E. (2009). **Oestradiol decreases colonic permeability through oestrogen receptor beta-mediated up-regulation of occludin and junctional adhesion molecule-A in epithelial cells.** J Physiol 587, 3317-3328.

4. Carrillo-de-Albornoz, A., Figuero, E., Herrera, D., Cuesta, P., and Bascones-Martinez, A. (2012). **Gingival changes during pregnancy: III. Impact of clinical, microbiological, immunological and socio-demographic factors on gingival inflammation.** J Clin Periodontol 39, 272-283.

5. CB, K., and NF, B. (2006). **Women's health issues and their relationship to periodontitis.** J Am Dent Assoc 133, 323-329.

6. Cereijido, M., Contreras, R.G., Flores-Benitez, D., Flores-Maldonado, C., Larre, I., Ruiz, A., and Shoshani, L. (2007). **New diseases derived or associated with the tight junction.** Arch Med Res 38, 465-478.

7. Chi, B., Qi, M., and Kuramitsu, H.K. (2003). **Role of dentilisin in *Treponema denticola* epithelial cell layer penetration.** Res Microbiol 154, 637-643.

8. Cho, I., and Blaser, M.J. (2012). **The human microbiome: at the interface of health and disease.** Nat Rev Genet 13, 260-270.

9. Choi, Y.S., Kim, Y.C., Ji, S., and Choi, Y. (2014). **Increased bacterial invasion and differential expression of tight-junction proteins, growth factors, and growth factor receptors in periodontal lesions.** J Periodontol 85, e313-322.

10. Choi, Y.S., Kim, Y.C., Jo, A.R., Ji, S., Koo, K.-T., Ko, Y., and Choi, Y. (2013). ***Porphyromonas gingivalis* and dextran sodium sulfate induce periodontitis through the disruption of physical barriers.** Eur J Inflamm 11, 419-431.

11. Chotirmall, S.H., Greene, C.M., Oglesby, I.K., Thomas, W., O'Neill, S.J., Harvey, B.J., and McElvaney, N.G. (2010). **17Beta-estradiol inhibits IL-8 in cystic fibrosis by up-regulating secretory leucoprotease inhibitor.** Am J Respir Crit Care Med 182, 62-72.

17. Chun, J., Kim, K.Y., Lee, J.H., and Choi, Y. (2010). **The analysis of oral microbial communities of wild-type and toll-like receptor 2-deficient mice using a 454 GS FLX Titanium pyrosequencer.** Bmc Microbiol 10, 101.

18. Chun, J., Lee, J.H., Jung, Y., Kim, M., Kim, S., Kim, B.K., and Lim, Y.W. (2007). **EzTaxon: a web-based tool for the identification of prokaryotes based on 16S ribosomal RNA gene sequences.** Int J Syst Evol Microbiol 57, 2259-2261.

19. Dale, B.A., and Fredericks, L.P. (2005). **Antimicrobial peptides in the oral environment: expression and function in health and disease.** Curr Issues Mol Biol 7, 119-133.

20. Dethlefsen, L., McFall-Ngai, M., and Relman, D.A. (2007). **An ecological and evolutionary perspective on human-microbe mutualism and disease.** Nature 449, 811-818.

21. Devlin, T.M., and Wiley-Liss, H. (2006). **Textbook of biochemistry with clinical correlations (6th Edition)**.

22. Dickman, K.G., Hempson, S.J., Anderson, J., Lippe, S., Zhao, L., Burakoff, R., and Shaw, R.D. (2000). **Rotavirus alters paracellular permeability and energy metabolism in Caco-2 cells.** Am J Physiol Gastrointest Liver Physiol 279, G757-G766.

23. Dorfel, M.J., and Huber, O. (2012). **Modulation of tight junction structure and function by kinases and phosphatases targeting occludin.** J Biomed Biotechnol, 2012, 8075356.

24. Edwards, P.C., and Kelsch, R. (2002). **Oral lichen planus: clinical presentation and management.** J Can Dent Assoc 68, 494-499.

25. Esposito, G. (1991). **Estriol: a weak estrogen or a different hormone?** Gynecol Endocrinol 5, 131-153.

26. Feng, Z., and Weinberg, A. (2006). **Role of bacteria in health and disease of periodontal tissues.** Periodontol 2000 40, 50-76.

27. Foster, J.S., and Kolenbrander, P.E. (2004). **Development of a multispecies oral bacterial community in a saliva-conditioned flow cell.** Appl Environ Microbiol 70, 4340-4348.

28. Franke, W.W., and Pape, U.F. (2012). **Diverse types of junctions containing tight junction proteins in stratified mammalian epithelia.** Ann N Y Acad Sci 1257, 152-157.

29. Galimanas, V., Hall, M.W., Singh, N., Lynch, M.D., Goldberg, M., Tenenbaum, H., Cvitkovitch, D.G., Neufeld, J.D., and Senadheera, D.B. (2014). **Bacterial community composition of chronic periodontitis and novel oral sampling sites for detecting disease indicators.** Microbiome 2, 32.

30. Giepmans, B.N., and van Ijzendoorn, S.C. (2009). **Epithelial cell-cell junctions and plasma membrane domains.** Biochim Biophys Acta 4, 820-831.

31. Gonzalez-Mariscal, L., Tapia, R., and Chamorro, D. (2008). **Crosstalk of tight junction components with signaling pathways.** Biochim Biophys Acta 3, 729-756.

32. Griffen, A.L., Beall, C.J., Campbell, J.H., Firestone, N.D., Kumar, P.S., Yang, Z.K., Podar, M., and Leys, E.J. (2012). **Distinct and complex bacterial profiles in human periodontitis and health revealed by 16S pyrosequencing.** ISME J 6, 1176-1185.

33. Haas, A.N., Rosing, C.K., Oppermann, R.V., Albandar, J.M., and Susin, C. (2009). **Association among menopause, hormone replacement therapy, and periodontal attachment loss in southern Brazilian women.** J Periodontol 80, 1380-1387.

34. Hajishengallis, G., Liang, S., Payne, M.A., Hashim, A., Jotwani, R., Eskan, M.A., McIntosh, M.L., Alsam, A., Kirkwood, K.L., Lambris, J.D., et al. (2011). **Low-abundance biofilm species orchestrates inflammatory periodontal disease through the commensal microbiota and complement.** Cell Host Microbe 10, 497-506.

35. Hamady, M., Lozupone, C., and Knight, R. (2010). **Fast UniFrac: facilitating high-throughput phylogenetic analyses of microbial communities including analysis of pyrosequencing and PhyloChip data.** ISME J 4, 17-27.

36. Hanin, A., Sava, I., Bao, Y., Huebner, J., Hartke, A., Auffray, Y., and Sauvageot, N. (2010). **Screening of in vivo activated genes in *Enterococcus faecalis* during insect and mouse infections and growth in urine.** PLoS ONE 5, e11879.

37. Hartsock, A., and Nelson, W.J. (2008). **Adherens and tight junctions: structure, function and connections to the actin cytoskeleton.** Biochim Biophys Acta 3, 660-669.

38. Hatakeyama, S., Yaegashi, T., Oikawa, Y., Fujiwara, H., Mikami, T., Takeda, Y., and Satoh, M. (2006). **Expression pattern of adhesion molecules in junctional epithelium differs from that in other gingival epithelia.** J Periodontal Res 41, 322-328.

39. Himmel, M.E., Crome, S.Q., Ivison, S., Piccirillo, C., Steiner, T.S., and Levings, M.K. (2011). **Human $CD4^+$ $FOXP3^+$ regulatory T cells produce CXCL8 and recruit neutrophils.** Eur J Immunol 41, 306-312.

41. Holt, S.C., Kesavalu, L., Walker, S., and Genco, C.A. (1999). **Virulence factors of *Porphyromonas gingivalis*.** Periodontolo 2000 20, 168-238.

42. Huber, T., Faulkner, G., and Hugenholtz, P. (2004). **Bellerophon: a program to detect chimeric sequences in multiple sequence alignments.** Bioinformatics 20, 2317-2319.

43. Iijima, W., Ohtani, H., Nakayama, T., Sugawara, Y., Sato, E., Nagura, H., Yoshie, O., and Sasano, T. (2003). **Infiltrating CD8$^+$ T cells in oral lichen planus predominantly express CCR5 and CXCR3 and carry respective chemokine ligands RANTES/CCL5 and IP-10/CXCL10 in their cytolytic granules.** Am J Pathol 163, 261-268.

44. Ishihara, K., and Okuda, K. (1999). **Molecular pathogenesis of the cell surface proteins and lipids from *Treponema denticola*.** FEMS Microbiol Lett 181, 199-204.

45. Ismail, S.B., Kumar, S.K.S., and Zain, R.B. (2007). **Oral lichen planus and lichenoid reactions: etiopathogenesis, diagnosis, management and malignant transformation.** J Oral Sci 49, 89-106.

46. JB, M., CM, S., and AJ, P. (1984). **Oral lichen planus: an immunoperoxidase study using monoclonal antibodies to lymphocyte subsets.** Br J Dermatol 111, 587-595.

47. Ji, S., Choi, Y.S., and Choi, Y. (2014). **Bacterial invasion and persistence: critical events in the pathogenesis of periodontitis?** J Periodontal Res 50, 570-585.

48. Ji, S., Hyun, J., Park, E., Lee, B.L., Kim, K.K., and Choi, Y. (2007). **Susceptibility of various oral bacteria to antimicrobial peptides and to phagocytosis by neutrophils.** J Periodontal Res 42, 410-419.

49. Kalaitzidis, D., and Gilmore, T.D. (2005). **Transcription factor cross-talk: the estrogen receptor and NF-kappaB.** Trends Endocrinol Metab 16, 46-52.

50. Katz, J., Yang, Q.B., Zhang, P., Potempa, J., Travis, J., Michalek, S.M., and Balkovetz, D.F. (2002). **Hydrolysis of epithelial junctional proteins by *Porphyromonas gingivalis* gingipains.** Infect Immun 70, 2512-2518.

51. Kim, Y.C., Ko, Y., Hong, S.D., Kim, K.Y., Lee, Y.H., Chae, C., and Choi, Y. (2010). **Presence of *Porphyromonas gingivalis* and plasma cell dominance in gingival tissues with periodontitis.** Oral Dis 16, 375-381.

52. Kimura, K., Teranishi, S., Fukuda, K., Kawamoto, K., and Nishida, T. (2008). **Delayed disruption of barrier function in cultured human corneal epithelial cells induced by tumor necrosis factor-alpha in a manner dependent on NF-kappaB.** Invest Ophthalmol Vis Sci 49, 565-571.

53. Kolaczkowska, E., and Kubes, P. (2013). **Neutrophil recruitment and function in health and inflammation.** Nat Rev Immunol 13, 159-175.

54. Kolenbrander, P.E., Palmer, R.J., Jr., Periasamy, S., and Jakubovics, N.S. (2010). **Oral multispecies biofilm development and the key role of cell-cell distance.** Nat Rev Microbiol 8, 471-480.

55. Konradt, C., Frigimelica, E., Nothelfer, K., Puhar, A., Salgado-Pabon, W., di Bartolo, V., Scott-Algara, D., Rodrigues, C.D., Sansonetti, P.J., and Phalipon, A. (2011). **The *Shigella flexneri* type three secretion system effector IpgD inhibits T cell migration by manipulating host phosphoinositide metabolism.** Cell Host Microbe 9, 263-272.

56. Kwak, Y.K., Vikstrom, E., Magnusson, K.E., Vecsey-Semjen, B., Colque-Navarro, P., and Mollby, R. (2012). **The *Staphylococcus aureus* alpha-toxin perturbs the barrier function in Caco-2 epithelial cell monolayers by altering junctional integrity.** Infect Immun 80, 1670-1680.

57. Lamont, R.J., Chan, A., Belton, C.M., Izutsu, K.T., Vasel, D., and Weinberg, A. (1995). ***Porphyromonas gingivalis* invasion of gingival epithelial cells.** Infect Immun 63, 3878-3885.

58. Lamont, R.J., and Yilmaz, O. (2002). **In or out: the invasiveness of oral bacteria.** Periodontol 2000 30, 61-69.

59. Listgarten, M.A. (1988). **A rationale for monitoring the periodontal microbiota after periodontal treatment.** J Periodontol 59, 439-444.

60. Liu, R., Wen, Y., Perez, E., Wang, X., Day, A.L., Simpkins, J.W., and Yang, S.H. (2005). **17beta-Estradiol attenuates blood-brain barrier disruption induced by cerebral ischemia-reperfusion injury in female rats.** Brain Res 1060, 55-61.

61. Loe, H., Anerud, A., Boysen, H., and Smith, M. (1978). **The natural history of periodontal disease in man. Study design and baseline data.** J Periodontal Res 13, 550-562.

62. Looijer-van Langen, M., Hotte, N., Dieleman, L.A., Albert, E., Mulder, C., and Madsen, K.L. (2011). **Estrogen receptor-beta signaling modulates epithelial barrier function.** Am J Physiol Gastrointest Liver Physiol 300, G621-626.

63. Lux, R., Miller, J.N., Park, N.H., and Shi, W.Y. (2001). **Motility and chemotaxis in tissue penetration of oral epithelial cell layers by *Treponema denticola*.** Infect Immun 69, 6276-6283.

64. Madianos, P.N., Papapanou, P.N., Nannmark, U., Dahlen, G., and Sandros, J. (1996). ***Porphyromonas gingivalis*** **FDC381 multiplies and persists within human oral epithelial cells in vitro.** Infect Immun 64, 660-664.

65. Masuda, K., and Kawata, T. (1982). **Isolation, properties, and reassembly of outer sheath carrying a polygonal array from an oral treponeme.** J bacteriol 150, 1405-1413.

66. Matthews, J.B., Wright, H.J., Roberts, A., Cooper, P.R., and Chapple, I.L. (2007). **Hyperactivity and reactivity of peripheral blood neutrophils in chronic periodontitis.** Clin Exp Immunol 147, 255-264.

67. McParland, H., and Warnakulasuriya, S. (2012). **Oral lichenoid contact lesions to mercury and dental amalgam-a review.** J Biomed Biotechnol 2012, 589569.

68. Meyer, D.H., Lippmann, J.E., and Fives-Taylor, P.M. (1996). **Invasion of epithelial cells by *Actinobacillus actinomycetemcomitans*: a dynamic, multistep process.** Infect Immun 64, 2988-2997.

69. Mishima, E., and Sharma, A. (2011). ***Tannerella forsythia* invasion in oral epithelial cells requires phosphoinositide 3-kinase activation and clathrin-mediated endocytosis.** Microbiology 157, 2382-2391.

70. Murakami, Y., Masuda, T., Imai, M., Iwami, J., Nakamura, H., Noguchi, T., and Yoshimura, F. (2004). **Analysis of major virulence factors in *Porphyromonas gingivalis* under various culture temperatures using specific antibodies.** Microbiol Immunol 48, 561-569.

71. Nakayama, K. (2003). **Molecular genetics of *Porphyromonas gingivalis*: gingipains and other virulence factors.** Curr Protein Pept Sci 4, 389-395.

72. Niessen, C.M. (2007). **Tight junctions/adherens junctions: basic structure and function.** J Invest Dermatol 127, 2525-2532.

73. Njoroge, T., Genco, R.J., Sojar, H.T., Hamada, N., and Genco, C.A. (1997). **A role for fimbriae in *Porphyromonas gingivalis* invasion of oral epithelial cells.** Infect Immun 65, 1980-1984.

74. Norman, A.W., Mizwicki, M.T., and Norman, D.P. (2004). **Steroid-hormone rapid actions, membrane receptors and a conformational ensemble model.** Nat Rev Drug Discov 3, 27-41.

75. Nusrat, A., von Eichel-Streiber, C., Turner, J.R., Verkade, P., Madara, J.L., and Parkos, C.A. (2001). ***Clostridium difficile* toxins disrupt epithelial barrier function by altering membrane microdomain localization of tight junction proteins.** Infect Immun 69, 1329-1336.

76. Nussbaum, G., and Shapira, L. (2011). **How has neutrophil research improved our understanding of periodontal pathogenesis?** J Clin Periodontol 38 Suppl 11, 49-59.

77. Nussdorfer, G.G., Rossi, G.P., Malendowicz, L.K., and Mazzocchi, G. (1999). **Autocrine-paracrine endothelin system in the physiology and pathology of steroid-secreting tissues.** Pharmacol Rev 51, 403-438.

78. Oh, T.J., Eber, R., and Wang, H.L. (2002). **Periodontal diseases in the child and adolescent.** J Clin Periodontol 29, 400-410.

79. Omar, A.A., Hietanen, J., Kero, M., Lukinmaa, P.L., and Hagstrom, J. (2009). **Oral lichen planus and chronic junctional stomatitis: differences in lymphocyte subpopulations.** Acta Odontol Scand 67, 366-369.

80. Page, R.C. (1986). **Gingivitis.** J Clin Periodontol 13, 345-359.

81. Park, O.J., Yi, H., Jeon, J.H., Kang, S.S., Koo, K.T., Kum, K.Y., Chun, J., Yun, C.H., and Han, S.H. (2015). **Pyrosequencing Analysis of Subgingival Microbiota in Distinct Periodontal Conditions.** J Dent Res 94, 921-927.

82. Pflughoeft, K.J., and Versalovic, J. (2012). **Human microbiome in health and disease.** Annu Rev Pathol 7, 99-122.

83. Roberts, F.A., and Darveau, R.P. (2002). **Beneficial bacteria of the periodontium.** Periodontol 2000 30, 40-50.

84. Salgado-Pabón, W., Celli, S., Arena, E.T., Nothelfer, K., Roux, P., Sellge, G., Frigimelica, E., Bousso, P., Sansonetti, P.J., and Phalipon, A. (2013). ***Shigella* impairs T lymphocyte dynamics in vivo.** Proc Natl Acad Sci U S A 110, 4458-4463.

85. Salim, S.Y., and Soderholm, J.D. (2011). **Importance of disrupted intestinal barrier in inflammatory bowel diseases.** Inflamm Bowel Dis 17, 362-381.

86. Schaefer, T.M., Wright, J.A., Pioli, P.A., and Wira, C.R. (2005). **IL-1beta-mediated proinflammatory responses are inhibited by estradiol via down-regulation of IL-1 receptor type I in uterine epithelial cells.** J Immunol 175, 6509-6516.

87. Sela, M.N. (2001). **Role of *Treponema denticola* in periodontal diseases.** Crit Rev Oral Biol Med 12, 399-413.

88. Sharma, A. (2010). **Virulence mechanisms of *Tannerella forsythia*.** Periodontol 2000 54, 106-116.

89. Shin, J., and Choi, Y. (2012). **The fate of *Treponema denticola* within human gingival epithelial cells.** Mol Oral Microbiol 27, 471-482.

90. Socransky, S.S., Haffajee, A.D., Cugini, M.A., Smith, C., and Kent, R.L., Jr. (1998). **Microbial complexes in subgingival plaque.** J Clin Periodontol 25, 134-144.

91. Spratt, D.A., Greenman, J., and Schaffer, A.G. (1995). ***Capnocytophaga gingivalis* aminopeptidase: A potential virulence factor.** Microbiol-Uk 141, 3087-3093.

92. Sugerman, P., and Savage, N. (2002). **Oral lichen planus: Causes, diagnosis and management.** Aust Dent J 47, 290-297.

93. Sumanasekera, W.K., Sumanasekera, G.U., Mattingly, K.A., Dougherty, S.M., Keynton, R.S., and Klinge, C.M. (2007). **Estradiol and dihydrotestosterone regulate endothelial cell barrier function after hypergravity-induced alterations in MAPK activity.** Am J Physiol Cell Physiol 293, C566-573.

94. Sumanasekera, W.K., Zhao, L., Ivanova, M., Morgan, D.D., Noisin, E.L., Keynton, R.S., and Klinge, C.M. (2006). **Effect of estradiol and dihydrotestosterone on hypergravity-induced MAPK signaling and occludin expression in human umbilical vein endothelial cells.** Cell Tissue Res 324, 243-253.

95. Tarkkila, L., Kari, K., Furuholm, J., Tiitinen, A., and Meurman, J.H. (2010). **Periodontal disease-associated micro-organisms in peri-menopausal and post-menopausal women using or not using hormone replacement therapy. A two-year follow-up study.** BMC Oral Health 10, 10.

96. Thornhill, M.H., Sankar, V., Xu, X.-J., Barrett, A.W., High, A.S., Odell, E.W., Speight, P.M., and Farthing, P.M. (2006). **The role of histopathological characteristics in distinguishing amalgam-associated oral lichenoid reactions and oral lichen planus.** J Oral Pathol Med 35, 233-240.

97. Valimaa, H., Savolainen, S., Soukka, T., Silvoniemi, P., Makela, S., Kujari, H., Gustafsson, J.A., and Laine, M. (2004). **Estrogen receptor-beta is the predominant estrogen receptor subtype in human oral epithelium and salivary glands.** J Endocrinol 180, 55-62.

98. Wade, W.G. (2013). **The oral microbiome in health and disease.** Pharmacol Res 69, 137-143.

99. Wang, Y., Zhang, J., Yi, X.J., and Yu, F.S.X. (2004). **Activation of ERK1/2 MAP kinase pathway induces tight junction disruption in human corneal epithelial cells.** Exp Eye Res 78, 125-136.

100. Wierman, M.E. (2007). **Sex steroid effects at target tissues: mechanisms of action.** Adv Physiol Educ 31, 26-33.

101. Wu, Z., Nybom, P., and Magnusson, K.-E. (2000). **Distinct effects of *Vibrio cholerae* haemagglutinin/ protease on the structure and localization of the tight junction-associated proteins occludin and ZO-1.** Cell Microbiol 2, 11-17.

102. Xing, D., Nozell, S., Chen, Y.F., Hage, F., and Oparil, S. (2009). **Estrogen and mechanisms of vascular protection.** Arterioscler Thromb Vasc Biol 29, 289-295.

103. Yang, N.J., Seol, D.W., Jo, J., Jang, H.M., Yoon, S.Y., and Lee, D.R. (2014). **Effect of cell-penetrating peptide-conjugated estrogen-related**

receptor beta on the development of mouse embryos cultured in vitro. Clin Exp Reprod Med 41, 1-8.

104. Yilmaz, O., Watanabe, K., and Lamont, R.J. (2002). **Involvement of integrins in fimbriae-mediated binding and invasion by *Porphyromonas gingivalis*.** Cell Microbiol 4, 305-314.

국문초록

목 적

구강편평태선은 T 세포의 면역반응에 의해 발생하는 원인이 알려지지 않은 피부점막 질환이다. 감염원, 약물, 자기 항원, 치과 재료, 항원에 대한 CD8 양성 림프구의 특이적인 면역 반응 등의 여러 가지 요인이 연관된 것으로 의심되고 있지만 정확한 질병의 원인이나 병인기전은 알려져 있지 않다.

숙주에 공생하는 세균은 숙주의 다양한 생리적 과정에 밀접한 관련이 있다. 이러한 세균 조성의 변화는 다양한 국소 혹은 전신 질환과 관련된 것으로 알려져 있다. 하지만 구강편평태선의 병인기전에서 구강 세균의 역할은 알려져 있지 않다.

에스트로겐은 물리적 장벽, 숙주의 면역반응 조절과 같은 상피의 항상성 유지에서 중요한 역할을 한다고 알려져 있다. 하지만, 치은상피의 항상성에 대한 에스트로겐의 역할은 알려져 있지 않다.

본 연구에서는 구강편평태선에서 세균의 역할과 에스트라디올의 치은상피 항상성 조절 효과를 규명하는 연구를 진행하였다.

방 법

구강편평태선 환자의 병변으로 침투된 세균를 확인하기 위해서, 구강편평태선 환자 (n=36) 와 비교 그룹 (n=10)의 구강점막 조직을 획득하였다. H&E 염색과 세균의 16S ribosomal RNA를 검출할 수 있는 프로브를 이용한 가시적 분자 결합화를 통해 세균을 검출하였다. 염증세포의 표지자들에 대한 항체를 이용하여 면역 조직

화학법을 시행한 후, 서열상관분석을 이용하여 침투된 세균과의 상관관계를 확인하였다. 또한, 조직 내에서 염증세포로의 세균의 침투를 확인하기 위해서, 세균의 검출과 CD8의 염색을 이중 검출하였다. 구강편평태선 환자 그룹과 정상 그룹의 구강 점막 세균의 조성을 비교하기 위해서, 구강편평태선 환자 (n=13) 와 비교 그룹 (n=18)의 볼과 입술의 점막 조직에서 구강세균을 채취하여, 파이로시퀀싱을 진행하였다.

림프구로 세균의 침투를 확인하기 위해서, 분리한 사람의 CD4, CD8, CD14 양성세포에 5-(and6-) carboxy-fluorescein diacetate succinimidyl ester (CFSE)로 염색된 세균을 감염시킨 후, 유세포분석기와 공초점현미경을 통해 관찰하였다. 염증세포 내 세균의 생존을 확인하기 위해서, 항생제 보호 분석법을 수행하였다. 또한, 세균에 의한 케모카인의 분비를 효소결합 면역흡착 분석법과 멀티플렉스 분석을 사용하여 분석하였다.

17-베타 에스트라디올이 치은상피세포의 물리적 장벽에 미치는 영향을 확인하기 위해서, 치은상피세포 단층에 17-베타 에스트라디올을 처리 하였다. 훼손이 없는 정상 조건에서 물리적 장벽의 기능을 TER (transepithelial electrical resistance) 분석하거나 혹은 전염증성 사이토카인으로 훼손을 준 조건에서 분석하였다. 또한, 밀착연접 단백질의 유전자와 단백질 발현을 실시간 역전사 중합효소 연쇄반응과 면역 조직 화학법을 이용하여 분석하였다. 또한, nuclear factor kappa-light-chain-enhancer of activated B cells (NF-κB)의 핵 내 이동을 면역 형광법을 이용하여 관찰하였다.

결 과

구강점막의 상피뿐만 아니라 점막고유층에서도 세균의 침투를 확인할 수 있었으며, 구강편평태선 환자의 점막고유층에서 세균의 침투가 통계적으로 유의하게 증가되었다. 점막고유층으로 침투된 세균은 CD4, CD8 림프구의 침윤과 통계적으로 유의하게 강한 양의 상관관계를 나타내었지만, 대식세포의 경우는 상관관계를 보이지 않았다. 또한, 세균의 표지를 CD8 양성 림프구와 음성 림프구에서 발견할 수 있었다.

구강편평태선 환자의 구강 점막 세균의 조성이 정상인의 세균 조성과 대체로 다르게 나타났다. 종 수준에서 관찰한 결과, 구강편평태선 환자와 정상인에서 42개의 세균이 통계적으로 유의하게 상대적 존재비의 차이를 보였다. 그 중 *Capnocytophaga gingivalis*는 구강편평태선의 위험도 증가와 통계적으로 유의하게 관련이 있음이 확인 되었다. *C. gingivalis*는 HOK (human oral keratinocytes) -16B cell의 생존 능력에 변화를 주지 않았지만, TER의 감소를 시간 의존적으로 유도하였다. 한 시간 감염 후에, 실험에 사용된 세균들이 모두 CD4, CD8, CD14 양성세포에서 관찰 되었다. 하지만 오직 *C. gingivalis*만 CD14 양성세포에서 24시간 후에 생존 하였다.

정상 상태에서 17-베타 에스트라디올은 상피의 물리적 장벽 강화와 밀착 연접 단백질의 증가를 유도하였다. 더욱이, 전염증성 사이토카인에 의해서 유도된 훼손 조건에서 17-베타 에스트라디올의 전처리는 밀착 연접 단백질의 발현 유지를 통해서 상피의 물리적 장벽 붕괴를 예방하였다. 또한, 17-베타 에스트라디올은 전염증성 사이토카인에 의해서 유도된 NF-κB의 핵 내 이동을 억제하였다.

결 론

점막 세포 혹은 점막 조직으로의 증가된 세균 침투와 변화된 세균의 조성이 구강편평태선 병인에서 원인이 될 수 있을 것이라고 사료된다. 또한, 17-베타 에스트라디올에 의한 상피 장벽의 유지가 조직 내 세균의 침투 예방과 구강편평태선 치료의 표적이 될 수 있을 것이라고 사료된다.

주요어: 구강편평태선, 물리적 장벽, 염증, 세균 침투, 항염증반응

학번: 2010-30658